PL-TR-94-2269

Characteristics of Rockbursts for Use in Seismic Discrimination

Theron J. Bennett
Margaret E. Marshall
Brian W. Barker
John R. Murphy

Maxwell Laboratories, Incorporated
S-CUBED Division
P. O. Box 1620
La Jolla, CA   92038-1620

DTIC
SELECTED
FEB 0 9 1995
B

19950206 183

January, 1994

Final Report
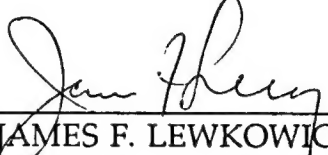(November, 1991 - October, 1993)

PHILLIPS LABORATORY
Directorate of Geophysics
AIR FORCE MATERIEL COMMAND
HANSCOM AIR FORCE BASE, MA 01731-3010

The views and conclusions contained in this document are those of the authors and should not be interpreted as representing the official policies, either express or implied, of the Air Force or the U.S. Government.

This technical report has been reviewed and is approved for publication.

JAMES F. LEWKOWICZ
Contract Manager
Earth Sciences Division

JAMES F. LEWKOWICZ, Director
Earth Sciences Division

This report has been reviewed by the ESC Public Affairs Office (PA) and is releasable to the National Technical Information Service (NTIS).

Qualified requestors may obtain additional copies from the Defense Technical Information Center. All others should apply to the National Technical Information Service.

If your address has changed, or if you wish to be removed from the mailing list, or if the addressee is no longer employed by your organization, please notify PL/TSI, 29 Randolph Road, Hanscom AFB, MA 01731-3010. This will assist us in maintaining a current mailing list.

Do not return copies of this report unless contractual obligations or notices on a specific document requires that it be returned.

REPORT DOCUMENTATION PAGE

1. AGENCY USE ONLY (Leave blank)	2. REPORT DATE	3. REPORT TYPE AND DATES COVERED	
	January, 1994	Final Report	11/91 - 10/93

4. TITLE AND SUBTITLE

Characteristics of Rockbursts for Use in Seismic Discrimination

6. AUTHOR(S)

Theron J. Bennett, Margaret E. Marshall, Brian W. Barker and John R. Murphy

5. FUNDING NUMBERS

Contract:
F19628-91-C-0186

PE 61102F
PR 2309
TA G2
WU BL

7. PERFORMING ORGANIZATION NAME(S) AND ADDRESS(ES)

Maxwell Laboratories, Inc.
S-CUBED Division
P.O. Box 1620
La Jolla, CA 92038-1620

8. PERFORMING ORGANIZATION REPORT NUMBER

SSS-FR-93-14382

9. SPONSORING/MONITORING AGENCY NAME(S) AND ADDRESS(ES)

Phillips Laboratory
29 Randolph Road
Hanscom AFB, MA 01731-3010
Contract Manager: James F. Lewkowicz/GPEH

10. SPONSORING/MONITORING AGENCY REPORT NUMBER

PL-TR-94-2269

11. SUPPLEMENTARY NOTES ·

12a. DISTRIBUTION/AVAILABILITY STATEMENT

Approved for public release; distribution unlimited

12b. DISTRIBUTION CODE

13. ABSTRACT (Maximum 200 words)

As a result of changing emphases in nuclear explosion monitoring, alternative types of seismic sources have become significant. This research program was designed to investigate the identification of one such source type - rockbursts. Development of a reliable scheme to separate these sources from other events is important for CTBT and non-proliferation monitoring. Our research has found that rockbursts occur in many seismic and aseismic regions throughout the world. In many areas rockbursts are frequent and they may be large (M > 5). Seismic waveform databases were assembled for two geographical regions: Central Europe and South Africa. Discrimination analyses, including comparisons of time-domain and spectral measurements of signals for different source types, have been performed on selected events. Because of the nature of rockbursts, some traditional discriminants, such as those related to focal depth, cannot be used. The most promising characteristics of rockburst seismic signals for discrimination seem to be spectral behavior and complexity. With regard to evasion the predictability of rockburst occurrence and size may offer the potential for concealment of a small or decoupled nuclear explosion test.

14. SUBJECT TERMS

Seismic	Rockbursts	South Africa	Evasion
Discrimination	Earthquakes	Europe	

15. NUMBER OF PAGES
102

16. PRICE CODE

17. SECURITY CLASSIFICATION OF REPORT	18. SECURITY CLASSIFICATION OF THIS PAGE	19. SECURITY CLASSIFICATION OF ABSTRACT	20. LIMITATION OF ABSTRACT
Unclassified	Unclassified	Unclassified	Unlimited

Table of Contents

List of Illustrations

1. Introduction

1.1 Background

In the area of seismic monitoring of underground nuclear explosion testing, the focus of research has shifted over the years depending to some degree on the terms of existing treaties and changing political interests. Throughout the era of the Threshold Test Ban Treaty (TTBT), the greatest attention has been given to determining the size and character of rather large nuclear explosion tests for specific source areas. In recent years increased concern over reaching agreement on a Comprehensive Test Ban Treaty (CTBT) and in curbing proliferation of nuclear weapons has stimulated interest in seismic discrimination of nuclear weapons tests from other types of sources. Particularly important issues for CTBT and non-proliferation monitoring are extending discrimination capabilities to lower magnitude levels and into new geographic regions. A consequence of this change in emphasis is that different types of seismic sources begin to play a role in the discrimination problem. One such event type is rockbursts induced by mining activity.

Five types of seismic events are important to the discrimination problem: (1) underground nuclear explosions, (2) earthquakes, (3) mine or quarry blasts, (4) construction and accidental chemical blasts, and (5) rockbursts or tremors induced by mining. Traditionally seismic discrimination research has focussed on the first two of these source types. However, as the threshold of interest is pushed to lower levels, the other event types must also be considered. In many areas these alternate sources are frequent, in some cases they may be large (particularly for rockbursts), and they may occur anywhere in the world.

1

Therefore, a reliable scheme for monitoring a CTBT worldwide and potential nuclear weapons testing in proliferant countries must have the capability to distinguish these different event types.

1.2 Research Objectives and Observations

The research effort described here has been directed at improving understanding of the rockburst or mine tremor seismic source for use in discrimination. Some of the standard teleseismic discriminants would not be expected to be effective for rockbursts. The frequent occurrence of these kinds of events in mining areas throughout the world suggests that it would be useful to develop techniques to facilitate their identification. In Figure 1 we present a map of the locations of reported rockbursts or mine tremors, which were encountered in the course of our review of rockburst activity and mechanisms. It can be seen that these events have been reported from a broad range of tectonic regions some of which are seismically active and some of which are not. The only continent which appears to have escaped rockburst activity is South America, and that may just indicate a lack of reporting or failure to investigate this kind of activity.

For purposes of this study, the term "rockburst" is used in a broad sense to include any type of stress-release phenomenon which has been induced by mining activity and which results in emission of seismic signals. Thus, we take rockbursts to include mine tremors, collapses, mine bumps, outbursts, and other similar processes. These kinds of events are most often associated with mining in rock usually at substantial depth; but, in fact, they have also been known to occur in mining near or even at the earth's surface. During the mining process,

2
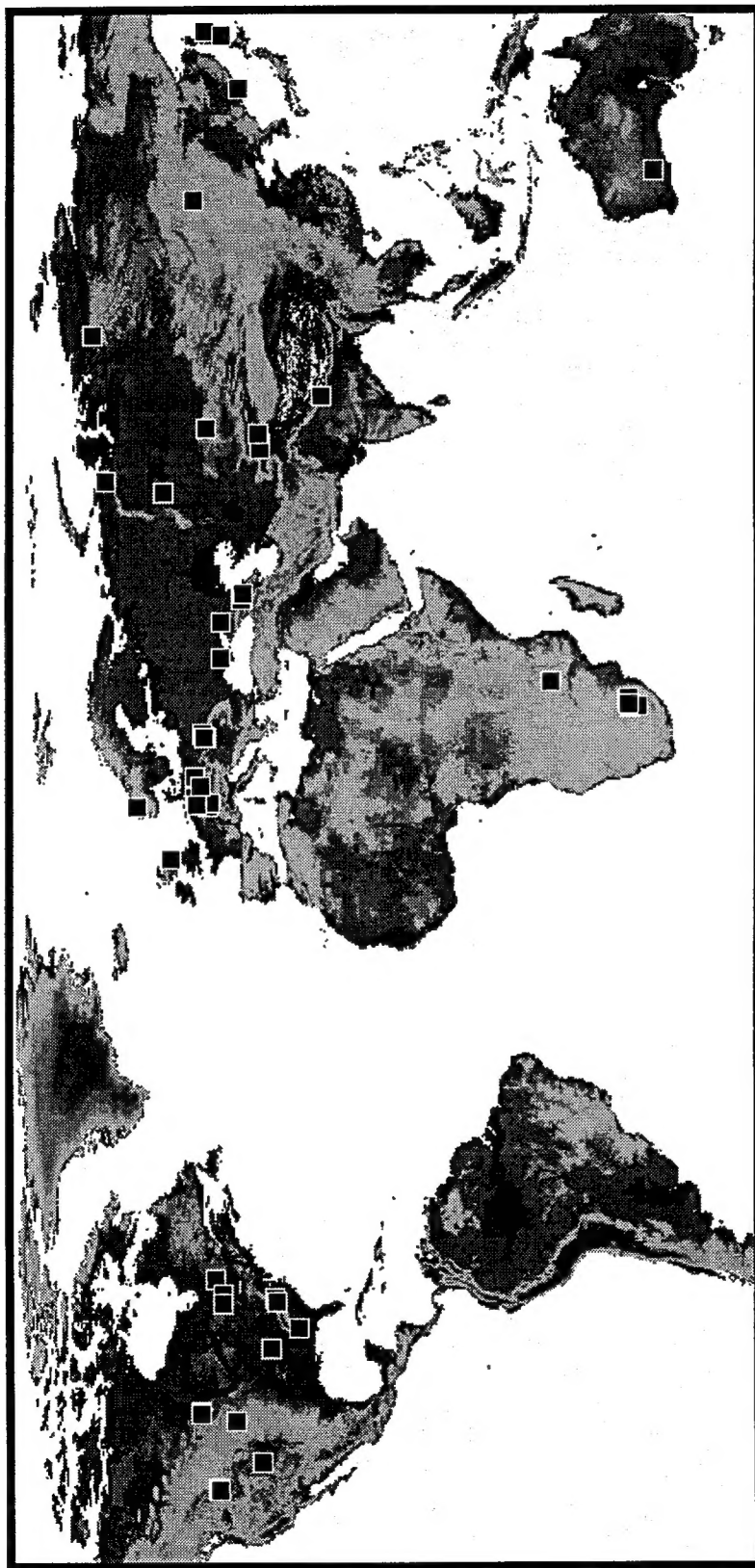
Figure 1. Locations of mining areas with reported rockbursts or tremors.

potential energy is added to the surrounding rock, which may already be prestressed due to the regional tectonic environment. This activity causes a readjustment of the surrounding stress field which then triggers the release of seismic energy. Thus, the occurrence of rockbursts in mines is dependent on the mining processes, including mine volume, rate of material removal, and support conditions, but also may be closely related to the regional tectonic stress and strength inhomogeneities in the surrounding rock.

The close association between rockbursts and tectonic stress implies that their mechanisms may resemble those of earthquakes. Many rockbursts indeed do appear to represent release of tectonic stress on preexisting zones of weakness or faults near the mine excavation and, therefore, the seismic field which they generate should be indistinct from that of an earthquake in the same region. However, some rockbursts are more complex including non-earthquake processes such as rock fall or pillar failure. Although one might expect that the seismic energy release in these latter events could not be great, we found that, in fact, one of the largest events which we encountered in our research appears to have been related to pillar failure, as will be described below.

One goal of mining engineering is to avoid hazardous conditions in removing ore, so we generally think of rockbursts as unusual events. However, in nearly all mining areas, the rockburst hazard has not been completely eliminated; and in some areas they may be quite frequent. The majority of rockbursts are small ($m_b < 3$); however, they occasionally (and in some cases regularly) exceed 5 m_b. In comparison, explosions connected with quarrying, strip mining, or construction at the earth's surface seldom have magnitudes greater than 3 - 4 m_b; and explosions used in development of underground

4

mines are usually in the magnitude range 1 - 3 m_b. Therefore, in many parts of the world mining-induced events may pose more of a problem to discrimination monitoring than commercial blasting operations.

The ultimate goal of discrimination research is to identify techniques to facilitate distinction of underground nuclear explosion tests from other event types. Some features of rockbursts suggest that they may behave like earthquakes in many aspects, but in some respects the behavior should be different. Rockbursts associated with induced slip along faults or fractures should behave like shallow earthquakes, and earthquake discrimination measures should be useful for their identification. However, rockbursts are shallow and in the same depth range as nuclear explosion tests; so depth discriminants will not generally be effective in separating them. Preliminary results described here suggest that, with respect to the M_S versus m_b discriminant measure, rockbursts may also tend to look explosion-like. However, we have identified features in the spectra of teleseismic signals, in the relative excitation of regional phases, and in the spectra of regional phases which appear to offer some promise for distinguishing rockbursts. We have also found evidence of complexity in the first motion patterns from rockbursts and in the signals themselves which may enable their distinction from nuclear explosion tests. Additional observations and theoretical studies are needed to test these results.

With regard to controllability of rockbursts and the potential for clandestine testing, our preliminary finding is that the feasibility of predicting the time and size of a rockburst event in a mining environment could provide an opportunity to conceal or disguise a clandestine nuclear explosion test. There

5

is evidence that rockbursts can be predicted and deliberately triggered in some mines. Questions regarding the maximum size of events which may be induced and the precision of timing predictions are still outstanding and require further study to reach a conclusion on this scenario.

1.3 Report Organization

The report is organized into six sections including this introduction. Section II describes the seismic databases, including rockbursts and contrasting source types, which we have assembled to evaluate rockburst characteristics and discrimination issues. The discrimination analyses which have been performed on teleseismic, far-regional and regional waveforms for Central European rockbursts and comparison event types are presented in Section III. Section IV describes similar discriminant analyses on the South African data. In Section V we review some additional discriminant measures and the implications of rockburst mechanisms for discrimination including potential problems posed by rockburst control for monitoring clandestine testing. Finally, Section VI summarizes our observations and provides some ideas for the direction of future investigations.

2. Seismic Database for Use in Rockburst Discrimination

2.1 Seismic Waveform Database Development

In our previous report (Bennett et al., 1993) we described the characteristics and conditions associated with rockbursts in different areas around the world. As noted there and in the introduction to this report, although some rockbursts or associated mine tremors are large, they are most often quite small and usually not very well recorded at normal seismic stations. At some mines local monitoring networks are used to keep track of mine tremors and warn of impending hazards to mining operations. However, in many countries there appears to be little special effort to account for rockburst occurrences and to separate them from other types of natural or man-made seismic activity. As a result, it is not an easy matter to assemble a waveform database of confirmed rockburst events. The problem is further complicated by the fact that mines where rockbursts occur may also use chemical explosions, so that location of an event at a mine alone does not distinguish between the possible source types.

The various complexities associated with database compilation led us to focus on two areas for our investigation of the seismic characteristics of rockbursts: Central Europe and South Africa. In both of these source regions, there have been frequent reports of rockbursts or mine tremors. In each area the maximum magnitudes of rockburst events have exceeded 5.0 m_b. Occurrence of large events permits analysis and comparisons of teleseismic signals from each source region. However, in each area there also exists some

7

regional monitoring capability which should enable extending the source characterizations to smaller events.

For both Central Europe and South Africa, it was not our goal to compile a complete database. The numerous events occurring in each area would make such a task impractical for a research project. We instead sought to select representative events which would be typical of rockbursts from each region which could then be characterized and compared with other types of sources. We also decided to consider first the larger events with reasonably good signal-to-noise conditions in the hope that characteristics, which might stand out at the higher signal-to-noise levels, could be extended to the smaller events where signals might be weak.

For each source region we relied on digital data available through CSS, IRIS, or AFTAC. Stations from which rockburst data have been compiled include SRO, ASRO, DWWSSN, ARPA regional arrays, Soviet IRIS, GSETT-2, and AEDS stations. Events which are included in the compilation produced good, visible signals at one or more of the stations whose waveforms we reviewed. For many of the smaller events, signals were frequently only usable from a single regional station, while some larger rockbursts produced strong teleseismic signals at ranges of 100 degrees or more. The data in our database usually includes all the available short-period and broad-band waveforms with sampling rates of 20 per second or higher. For regional signals we tried to retrieve waveform segments corresponding to group velocity windows from prior to P through Lg. We also retrieved long-period surface-wave data at one sample per second for many events.

In addition to the rockbursts from each source region, we attempted to include in our database other source types which could be used for comparisons. These other source types included both earthquakes and chemical blasts. Wherever possible an attempt was made to find events with similar magnitudes and locations to the rockbursts for use in the comparisons. Because coincident sources of different types were not usually available, we alternatively tried to pick events from the same tectonic region and at about the same epicentral distance range. We also compared characteristics of seismic signals between similar source types to help understand variability between events of a common type.

As we described in our previous report (cf. Bennett et al., 1993), it is only rarely that published information exists to corroborate events as rockbursts. In most cases the identification of events as rockbursts is based on inference derived from knowledge that the events occur in mining areas where rockbursts have been reported in the past and where natural seismicity was rare or unknown prior to the initiation of mining activity. In many cases the mining areas with inferred rockbursts are underground so that blasting is either not used in mine development or it involves very low energy release (i.e. smaller than many of the rockbursts). As a result, we believe it is unlikely that mineblasts or natural earthquakes are incorrectly designated as rockbursts for use in this study. Some surface quarrying or strip mining is believed to use larger blasts, but the sources of such events are usually fairly well-defined and frequently separate from the rockburst areas.

9

2.2 Central European Database

Our database for Central Europe consists of 60 events as shown in Table 1. These events include 48 rockbursts or mine tremors (either reported, rb, or probable rockbursts, prb), 7 earthquakes (eqk), 4 mineblasts (mb), and an accidental underground blast (b). A few small events had no reported magnitudes; for the remainder the magnitudes were in the range from 2.0 to 5.5 m_b. The majority of the rockbursts in the database had source locations in Poland although some also occurred in Germany. The earthquakes had epicenters in the Netherlands, Germany, Austria, and near the German/Czech border. Mineblasts had locations in Austria and near the German/Czech border and the Russian/Finnish border. The accidental underground blast occurred in Switzerland. The map in Figure 2 shows the locations of these 60 events.

The Polish rockbursts are clustered in two areas near the Czech border: one centered near 51.1°N, 15.8°E, and the other near 51.0°N 19.0°E. These correspond to the copper mining area near Lubin and a coal mining area in Upper Silesia respectively. Both areas have had long histories of mining-induced seismicity (cf. Gibowicz, 1984; Bennett et al., 1993). The largest German rockburst (5.4 m_b) has attracted considerable attention (cf. Ahorner, 1989; Minkley, 1993) and appears to have been associated with the extensive, nearly simultaneous collapse of multiple pillars in a mine near Völkershausen, as will be discussed more completely below. The large earthquake in the Netherlands (5.5 m_b) apparently had a hypocenter at middle to lower crustal depths (see below) and produced numerous aftershocks. Little is known about the reported mineblasts in the database except that they were generally quite small relative to the other events; they have been included to provide another

10

Table 1. Central European Events in Current Database

Date	Origin Time	Lat (N)	Lon (E)	Mag	ID
08/15/80	20:03:04	51.153	15.892	3.6	prb
08/25/80	00:40:48	51.115	15.745	3.3	prb
09/14/80	15:39:13	51.623	16.200	3.6	prb
09/30/80	01:02:00	50.350	18.910	-	prb
10/02/80	17:23:44	51.319	15.571	3.9	prb
10/09/80	04:46:59	51.095	15.687	3.4	prb
11/29/80	20:42:00	51.250	19.400	-	prb
12/21/80	05:51:16	51.633	16.259	4.2	prb
12/23/80	21:10:30	51.636	16.375	3.7	prb
04/10/81	04:59:47	51.630	16.180	4.3	prb
07/12/81	11:59:26	50.522	19.012	4.1	prb
08/02/81	03:25:16	50.254	18.779	-	prb
08/11/81	23:48:06	49.861	18.425	4.1	prb
08/15/81	05:40:14	51.457	15.954	4.0	prb
08/19/81	12:41:25	52.103	17.574	3.4	prb
09/23/81	23:53:41	51.153	15.818	2.8	prb
11/03/81	05:42:44	51.027	15.867	3.7	prb
11/25/81	10:14:20	51.055	15.828	3.9	prb
12/11/81	02:02:32	51.161	15.817	3.9	prb
01/16/82	11:15:59	51.610	16.281	4.2	prb
01/22/82	03:09:03	51.156	15.516	3.4	prb
03/19/82	14:48:05	50.988	15.155	3.3	prb
04/12/82	12:45:37	51.512	15.966	3.4	prb
04/18/82	06:42:16	51.651	16.085	3.5	prb
04/22/82	21:22:38	51.153	15.860	3.3	prb
05/23/82	18:22:41	50.851	15.158	3.3	prb
06/04/82	10:44:34	50.537	19.062	4.6	prb
06/08/82	15:48:29	51.444	15.961	4.0	prb
06/08/82	16:33:40	51.156	15.831	3.4	prb
06/13/82	21:15:27	51.689	15.946	4.1	prb
06/15/82	20:00:59	51.620	16.278	3.7	prb
06/17/82	09:30:42	49.915	18.470	3.8	prb
06/19/82	23:36:29	51.532	15.986	3.7	prb
07/14/82	00:56:37	51.681	16.098	4.0	prb
08/24/85	06:08:40	50.275	7.917	4.3	eqk
10/25/86	20:07:23	51.640	16.080	4.9	prb
05/31/87	02:54:27	51.600	16.270	4.9	prb
06/20/87	00:37:56	51.480	16.050	4.7	prb
03/13/89	13:12:15	50.710	9.900	5.4	rb
03/25/89	12:46:40	51.620	16.090	5.3	prb

Date	Origin Time	Lat (N)	Lon (E)	Mag	ID
06/29/89	17:33:51	51.438	16.120	4.7	prb
10/28/89	01:35:53	51.600	16.010	4.7	prb
11/29/90	12:29:11	60.914	29.131	2.7	mb
04/30/91	03:40:39	51.542	16.227	3.3	prb
05/02/91	10:15:20	47.962	16.204	4.3	eqk
05/16/91	02:06:17	52.281	7.761	4.4	prb
05/16/91	10:44:58	49.288	6.930	3.0	prb
05/19/91	03:22:13	50.312	12.441	2.8	eqk
05/21/91	16:49:09	50.260	19.220	3.1	prb
05/23/91	19:42:56	51.583	16.085	3.1	prb
05/26/91	11:01:01	50.140	12.850	2.1	mb
05/26/91	19:42:55	50.183	12.715	2.0	mb
05/28/91	03:52:50	51.528	16.392	3.4	prb
10/22/91	19:19:25	51.561	16.115	3.3	prb
04/13/92	01:20:05	51.374	6.133	5.5	eqk
04/13/92	03:49:41	51.043	5.910	3.8	eqk
04/13/92	06:02:10	51.099	5.885	3.7	eqk
04/14/92	01:06:46	50.748	6.039	4.3	eqk
07/03/92	07:53:01	47.500	14.900	-	mb
11/02/92	15:13:26	46.730	8.330	4.2	b
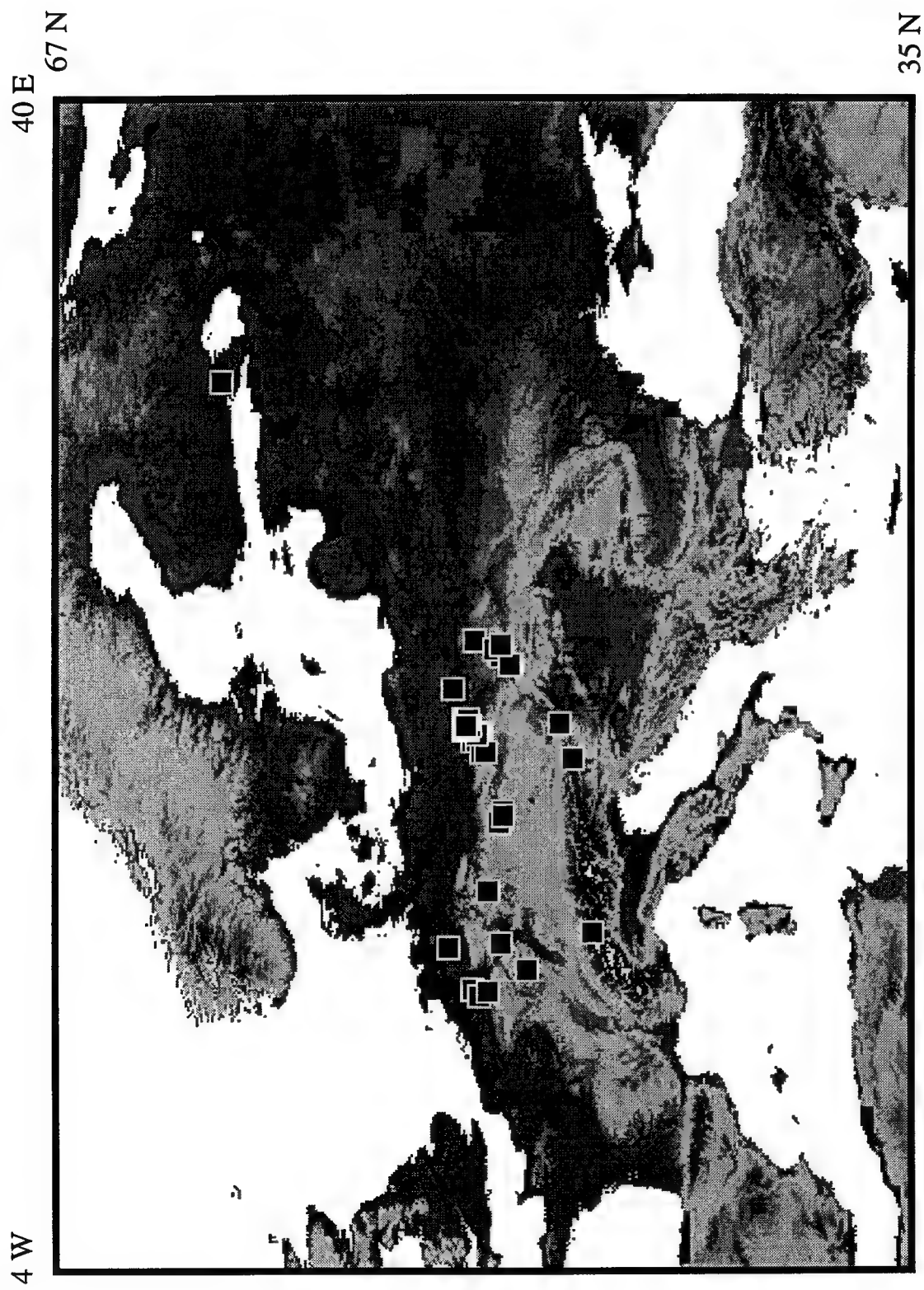
Figure 2. Map of event locations for the Central European database.

source type for signal comparisons. The accidental explosion in Switzerland had a magnitude of 4.2 m_b and was the result of the detonation of ammunition in a storage bunker. This event appears to be the largest blast in the recent history of Central Europe which has been well-recorded on high-quality seismic stations and thus provides another valuable comparison; however, little information about the source of this event has been published at this time.

In a previous report, Bennett et al. (1993) reviewed the general characteristics of seismic signals from events in Central Europe. The largest events produce strong body wave signals at teleseismic stations. However, many of the small rockbursts and mineblasts are not well recorded at teleseismic stations; and, therefore, regional signals are important to their identification. In this study we have performed discrimination analyses on data for several large Central European events recorded at teleseismic stations, including AEDS network stations. We have also done comparative analyses of different Central European event types at nearly common far-regional epicentral distances recorded at the ARPA regional array at NORESS. Finally, we have conducted more detailed discrimination analyses of several different types of smaller events recorded at about the same smaller regional distances, but different azimuths, from the GDSN station GRFO.

2.3 South African Database

Our database for South Africa includes 79 events (cf. Table 2). Except for a few events of unknown magnitude, the magnitudes are in the range from 2.3 to 5.5 M_L. The majority of the events (61) are thought to be rockbursts or mine tremors (prb) based on their location within the area of deep gold mining in the

14

Table 2. South African Events in Current Database

Date	Origin Time	Lat (S)	Lon (E)	Mag	ID
01/28/80	06:30:57	26.396	27.463	4.5	prb
02/09/80	13:51:10	27.802	26.235	5.2	prb
02/17/80	21:01:22	27.627	26.865	4.7	prb
03/22/80	02:14:10	26.120	27.752	5.2	prb
04/03/80	22:45:38	26.081	27.703	4.8	prb
04/08/80	00:39:35	26.293	27.653	4.2	prb
05/06/80	21:07:25	26.926	26.998	4.6	prb
06/12/80	03:03:42	26.991	26.991	4.8	prb
06/13/80	21:15:03	26.845	26.769	4.8	prb
01/28/81	16:20:33	26.073	27.611	4.6	prb
02/18/81	08:28:20	26.625	26.607	4.7	prb
07/07/81	12:52:42	26.552	27.026	4.2	prb
11/05/81	20:19:31	29.950	27.370	4.0	eqk
11/19/81	17:19:42	28.000	26.840	3.6	prb
11/22/81	03:31:27	26.400	27.500	3.6	prb
11/22/81	05:15:59	26.380	27.570	3.3	prb
11/26/81	07:16:49	24.080	30.980	3.2	eqk
12/01/81	09:04:34	25.207	27.912	3.3	prb
12/01/81	15:11:45	26.400	27.370	3.3	prb
12/14/81	14:41:01	26.320	27.330	4.0	prb
12/15/81	14:11:15	27.600	27.100	4.7	prb
12/15/81	16:29:49	26.360	27.530	3.0	prb
03/26/82	13:41:24	27.660	31.100	4.3	eqk
03/28/82	15:51:37	26.270	28.220	4.1	prb
04/01/82	07:11:01	30.040	19.400	3.4	eqk
04/02/82	12:57:09	26.830	26.750	3.2	prb
04/02/82	20:08:54	26.220	28.090	3.0	prb
04/09/82	01:52:37	26.800	26.600	3.9	prb
04/13/82	11:26:00	27.920	26.780	5.0	prb
04/13/82	11:26:51	27.900	26.800	4.6	prb
05/09/82	07:07:02	29.600	27.060	3.4	eqk
06/07/82	00:56:30	27.900	26.800	3.9	prb
06/16/82	17:57:22	23.500	26.100	-	eqk
06/17/82	04:18:52	26.140	27.710	-	prb
06/27/82	00:36:36	26.760	26.540	3.6	prb
06/28/82	09:20:08	26.880	26.810	3.4	prb
09/01/82	11:38:20	27.930	26.830	3.7	prb
09/10/82	09:24:21	26.200	29.900	-	eqk
11/12/82	06:11:32	26.906	26.750	5.0	prb
12/02/82	20:45:34	30.600	21.800	3.2	eqk

Date	Origin Time	Lat (S)	Lon (E)	Mag	ID
12/11/82	22:03:04	26.900	26.600	3.9	prb
12/11/82	22:03:59	26.830	26.720	3.8	prb
02/22/83	16:26:41	29.493	28.493	-	eqk
05/24/83	11:49:51	26.900	26.720	2.6	prb
05/24/83	13:09:57	27.990	26.800	3.2	prb
06/01/83	00:55:22	26.200	28.130	3.3	prb
06/03/83	16:13:59	26.220	28.150	2.3	prb
06/06/83	10:48:51	26.890	26.660	5.2	prb
07/17/83	13:38:07	26.140	27.890	2.8	prb
07/31/83	00:35:41	31.190	24.250	3.7	eqk
08/01/83	16:58:21	26.220	28.210	2.8	prb
08/04/83	06:05:48	33.390	19.270	-	eqk
08/26/83	21:19:26	30.830	21.500	2.7	eqk
08/26/83	21:29:49	26.350	27.320	2.7	prb
09/05/83	00:33:36	29.470	25.020	4.7	eqk
09/05/83	00:33:43	29.200	24.800	-	eqk
09/09/83	03:05:34	29.540	24.900	-	eqk
09/29/83	08:59:12	28.020	26.880	2.8	prb
10/01/83	04:43:13	26.190	27.700	-	prb
11/02/83	23:16:47	30.060	25.790	3.2	eqk
12/27/83	07:38:24	26.421	27.387	4.9	prb
01/28/84	14:40:02	26.900	26.650	4.9	prb
03/21/84	16:47:58	26.190	27.850	2.9	prb
06/04/84	06:45:07	20.140	26.250	3.5	eqk
08/11/84	21:23:10	26.800	26.520	4.9	prb
08/19/84	15:31:52	29.580	26.710	-	eqk
01/01/86	16:00:50	26.780	26.600	4.9	prb
02/10/86	20:45:02	27.940	26.750	5.0	prb
08/11/86	04:59:10	26.920	26.570	4.9	prb
09/15/86	07:06:31	26.270	27.430	4.9	prb
10/28/86	15:04:21	26.980	26.680	5.2	prb
12/29/86	20:41:59	26.304	27.486	4.8	prb
01/05/88	06:41:17	26.807	26.639	5.2	prb
01/25/89	10:14:33	27.985	26.734	5.5	prb
02/27/90	16:17:10	26.872	26.736	4.6	prb
09/26/90	23:08:24	28.014	26.727	5.4	prb
11/14/90	00:31:39	28.122	26.789	4.8	prb
11/03/91	18:28:55	26.895	26.700	5.1	prb
12/01/91	20:03:11	26.878	26.664	5.0	prb

Witwatersrand basin near 27°S 27°E. The remaining 18 events have locations outside this area and are, therefore, classified here as probable earthquakes (eqk), although in only a few cases does actual corroboration of the source type exist in the ISC Bulletin or South African Seismicity Bulletins. The map in Figure 3 shows the locations of the events in our South African database.

In our previous report (Bennett et al., 1993) we described some of the general characteristics of rockburst occurrence in the South African gold mining district. The induced activity there follows a somewhat arcuate trend coincident with the mine locations. There has been an abundance of reports in the scientific literature on the occurrence and mechanisms of South African rockbursts. The events are generally deep and frequent, with nearly 85 events per year in the magnitude range 3.4 to 5.9 M_L during the period 1971 to 1979. Because of the frequency and long history of induced seismicity and extensive monitoring program in South Africa, more is probably known about the mechanisms and relation of their occurrence to excavation operations there than in any other area. We will summarize the general state of understanding of South African rockburst mechanisms in a subsequent section of this report.

Bennett et al. (1993) noted that the best available GDSN data for South African rockbursts came from the regional station at SLR and from a few teleseismic stations, including BCAO in Central Africa and ZOBO in Bolivia, South America. In this report we have added valuable data from teleseismic AEDS network stations for several South African events. We will describe some parametric observations as well as spectral characteristics of the teleseismic AEDS station signals for these events. We have also performed additional discrimination analyses of the BCAO long-period data for several of the larger

17
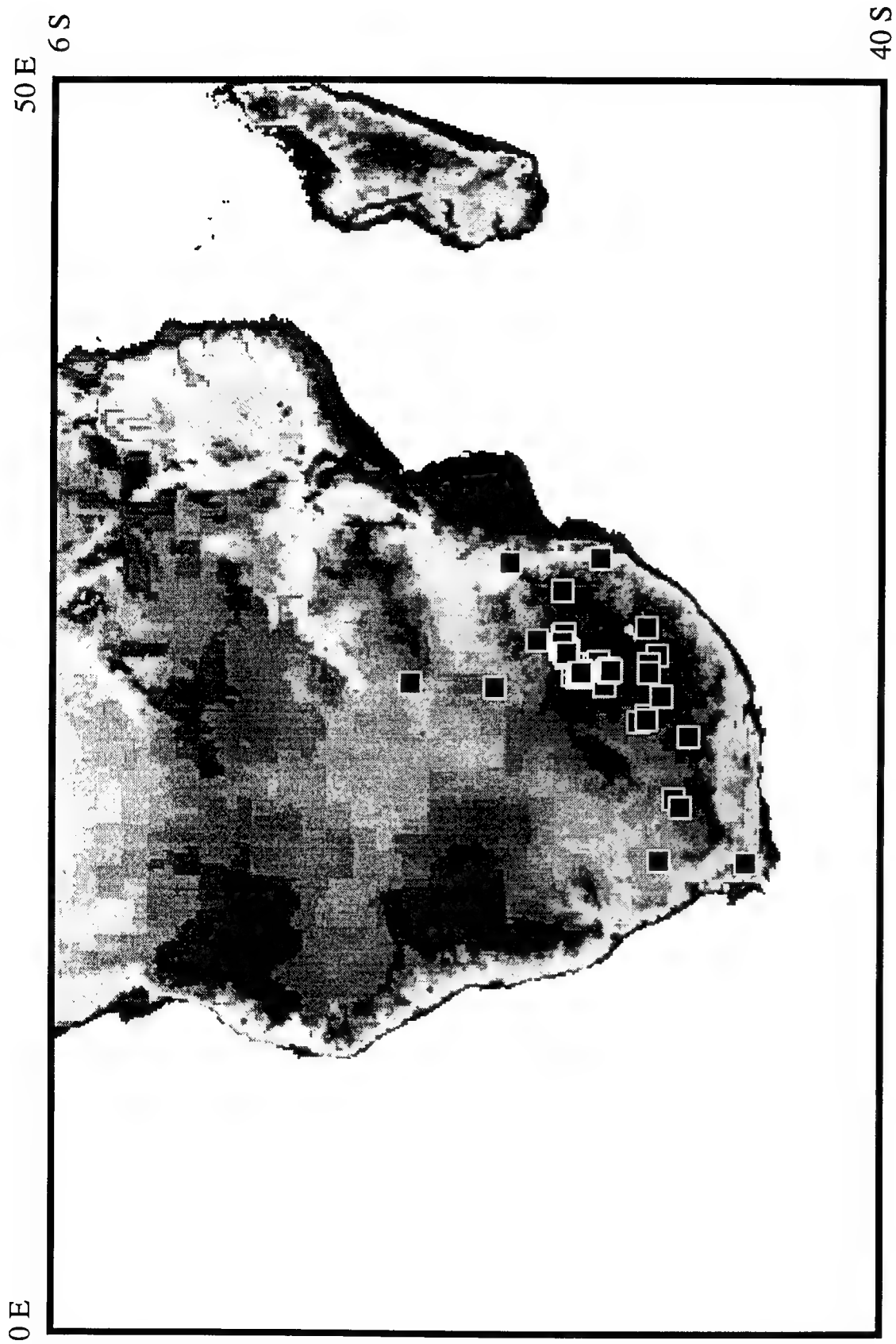
Figure 3. Map of event locations for the South African database.

events. As was the case for the larger Central European events at GRFO, large South African mine tremors frequently exceed the recording threshold at the nearby SLR station. Therefore, the near-regional monitoring effort for South African rockbursts must focus on smaller events. In a latter section we will summarize some of the characteristics of near regional signals from South African rockbursts based on the SLR observations and their relevance to discrimination.

3. Central European Events

3.1 Teleseismic Signals

We begin our analyses of Central European rockbursts with a comparison of teleseismic signals for three large Central European events recorded at AEDS stations. The events used in this comparison were the 4/13/92 Netherlands earthquake (5.5 m_b), the 3/13/89 German rockburst (5.4 m_b), and the 6/29/89 Polish rockburst (4.7 m_b). After reviewing the available waveform data, we selected the records from eight common AEDS stations for each event. The stations were at distances in the range $50° < \Delta < 80°$.

With regard to general teleseismic waveform features, the initial P waveforms for the rockbursts at common stations appear somewhat more complex than for the first earthquake P signals. At least two factors may contribute to the observed differences. Since the rockbursts are shallower than the earthquakes, site response of the shallow near-source crust may produce longer duration and complexity compared to the earthquake. A second factor is complexity of the mechanism. Some rockburst sources appear to be more complex including multiple events or episodes. In fact, comparison of the 3/13/89 rockburst P-wave signals with the 6/29/89 rockburst signals suggests that some rockbursts are more complex than others. The 3/13/89 rockburst appears to have a precursory phase arriving about two seconds prior to the main P at all the teleseismic AEDS stations. This phase is approximately one-third the amplitude of the main P phase. There are also indications in the rockburst record of two or more phases occurring after the main P within 5 - 6 seconds. Because the intervals of these multiple P phases appear to be nearly

20

the same at all stations (i.e. no evidence of moveout), it seems unlikely that they are caused by multiple mantle phases but are more probably produced by multiple events at the source. In fact, such complexity in the source of the 3/13/89 rockburst may explain some questions involved in interpreting the mechanism from P-wave first motions, as will be discussed in a subsequent section.

One other difference in the earthquake signals is the appearance of a rather strong depth phase. This phase arrives about 7.5 - 8 seconds after the initial P and is quite strong on the records at nearly all the AEDS stations. Assuming this phase to be pP the difference in time relative to P would indicate a source depth of about 20 km. This agrees with the source depth of 21 km reported by NEIC for the 4/13/92 Netherlands earthquake.

3.2 Spectral Comparisons of Teleseismic P

To develop a better understanding of possible spectral differences and variability in the P wave signals from rockbursts and other sources, we performed spectral analyses on the P signals at the AEDS stations for the 4/13/92 earthquake, the 3/13/89 rockburst, and the 6/29/89 rockburst. We analyze the results here in terms of the P/P spectral ratios between events as recorded at common stations. Thus, we represent the observed P-wave spectrum at a station as

$$A(\omega) = S_O(\omega)\, P_R(\omega)\, T_S(\omega) \qquad (1)$$

where $S_O(\omega)$ is the source spectrum (including source mechanism and source site response effects), $P_R(\omega)$ is a propagation path response, and $T_S(\omega)$ is the

21

station site and instrument transfer function. Then, for two different events the P/P spectral ratio is:

$$R_{P/P} \equiv \frac{A_1(\omega)}{A_2(\omega)} = \frac{S_{o1}(\omega)}{S_{o2}(\omega)} \frac{P_{R1}(\omega)}{P_{R2}(\omega)} \frac{T_{S1}(\omega)}{T_{S2}(\omega)} \qquad (2)$$

Since we are taking the ratios at common stations, $T_{S1} = T_{S2}$ and we will also assume that $P_{RI} \approx P_{R2}$ since all sources are in the same region and, therefore, have about the same transmission path to the common stations. Thus, the spectral ratio,

$$R_{P/P}(\omega) \approx \frac{S_{o1}(\omega)}{S_{o2}(\omega)} \qquad (3)$$

should provide an indication of source spectral differences between events.

For the Central European earthquake and rockbursts, we selected P-wave window segments 7.5 seconds long from each of eight teleseismic, common AEDS stations and a noise segment of similar duration from the time segment preceding P. Fourier spectra were computed for both the P and the noise segments corresponding to each waveform. Spectral bands in which signal-to-noise (S/N) ratios were strongest for each station and event were identified. For each common station we then computed the P/P spectral ratios for the 3/13/89 rockburst to the 4/13/92 earthquake and for the 6/29/89 rockburst to the 4/13/92 earthquake. The ratios were computed over the frequency band in which the S/N ratio was good (generally greater than one) at each station. The average P/P ratios over all the common stations were next computed using values of the ratios for which S/N was good. This last averaging process should further reduce any station effects which might persist in the ratios.

The average ratios with plus- and minus-one-sigma (± 1 σ) bounds about the mean ratios can then be compared. These are presented in Figure 4. At
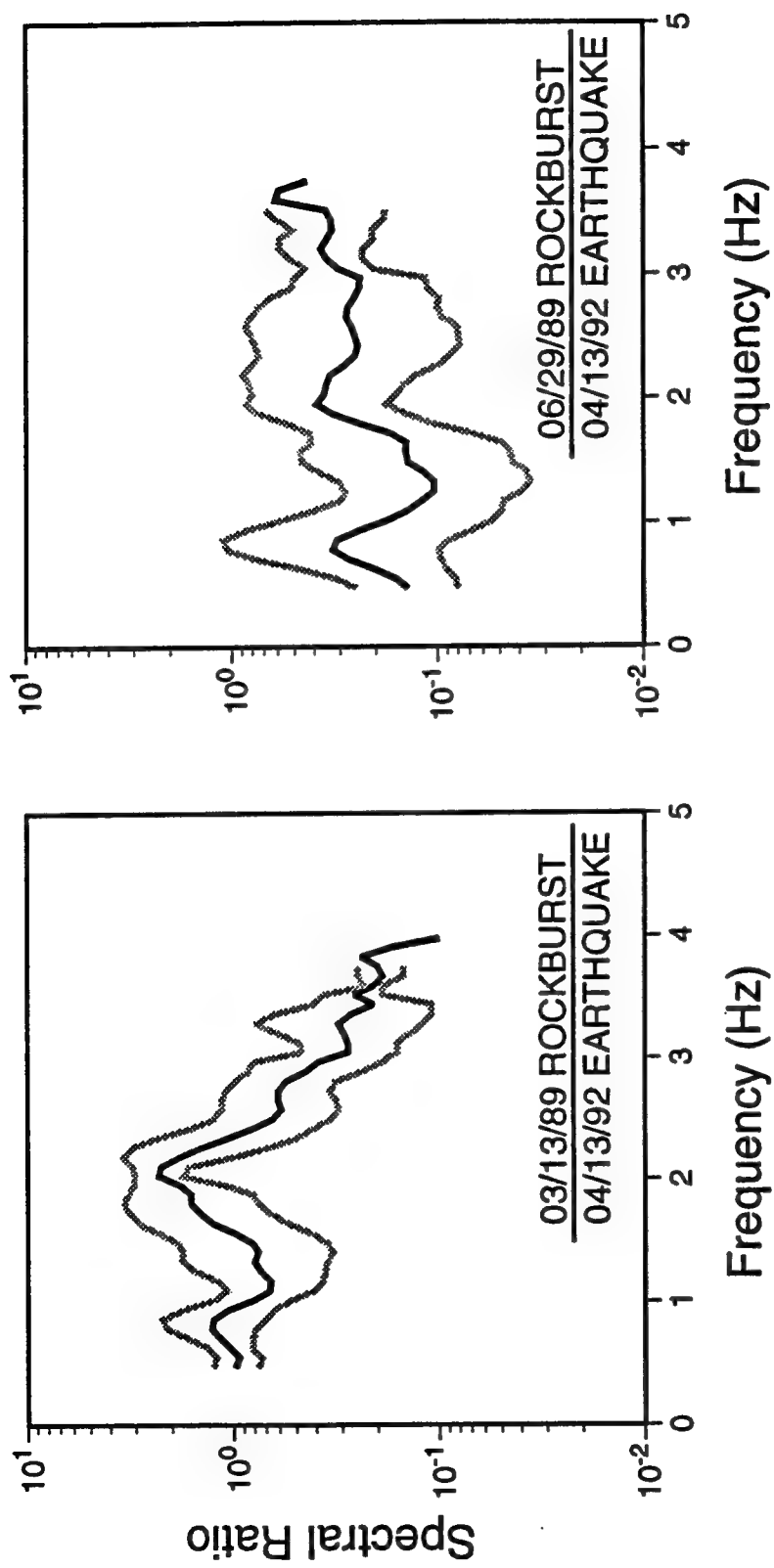
22

Figure 4. Average P/P spectral ratios and ±1σ bounds determined from teleseismic AEDS stations for large Central European rockbursts and the large Netherlands earthquake.

low frequencies (0.5 - 1.5 Hz) the P/P spectral ratios for 3/13/89 rockburst/4/13/92 earthquake is relatively flat and oscillates slightly around a value near 1.0. This is consistent with the comparable m_b values of the two events. The average ratio has a prominent peak near 2 Hz indicating enhancement of the rockburst P signal relative to the earthquake, or deficiency of the earthquake relative to the rockburst, within that band. Ignoring the peak near 2 Hz, the general behavior of the P/P spectral ratio appears to represent a rather steady decline toward higher frequencies, suggesting that the earthquake has more high-frequency P-wave energy than the rockburst.

For the 6/29/89 rockburst comparison to the 4/13/92 earthquake shown at the right of Figure 4, the P/P spectral ratios are generally lower. This is probably primarily indicative of the smaller magnitude of this rockburst event relative to the earthquake. The spectral ratio again shows some rather prominent peaks near 2 Hz and also near 0.8 Hz. Unlike the other example, however, the trend over the broader frequency band is generally upward toward higher frequencies. Several factors could be responsible for this difference in the spectral ratios. The increase with frequency observed for the 6/29/89 event might be explained partly by a shift toward higher corner frequency for the smaller event. An alternative explanation, which is probably most interesting from the standpoint of discrimination, is that the difference in mechanism between the German event (thought to have been a collapse) and the Polish rockburst (thought to have been more tectonic in character) is the source of the spectral differences. Two more-mundane explanations for the observed differences in behavior might be differences in the near-source site response

24

between the two rockbursts or some degree of noise contamination at higher frequencies in the spectrum for the smaller event.

Thus, the results of the teleseismic P-wave analyses for the Central European rockbursts are not so clear. There may be variability between events with some types of rockbursts (tectonic) tending to be enriched in higher frequencies compared to collapse type events. However, additional work is needed to resolve alternative explanations and tie-down source identification procedures. This work should include analyses of additional observations as well as theoretical investigations of variability in source mechanisms.

3.3 Far-Regional Signal Analyses

In addition to the teleseismic data, regional signals are expected to provide a valuable contribution to rockburst identification, particularly as events approach smaller magnitude levels. As part of our investigation of rockburst signal characteristics, we analyzed the behavior of several events, from the database described in Section II, recorded at far-regional stations. These analyses again focus on different event types recorded at common stations.

Figure 5 shows a map with the locations of three fairly large rockbursts and the large Netherlands earthquake in Central Europe along with the locations of three good far-regional stations which would be expected to provide good signals from the events. Figure 6 shows a comparison of the vertical-component signals recorded at these stations from the 3/13/89 German rockburst (5.4 m_b) and the 4/13/92 Netherlands earthquake (5.5 m_b). For the two events the distances to the individual stations are roughly comparable. Several differences are apparent in the time-domain signal behavior. At NRAO

25
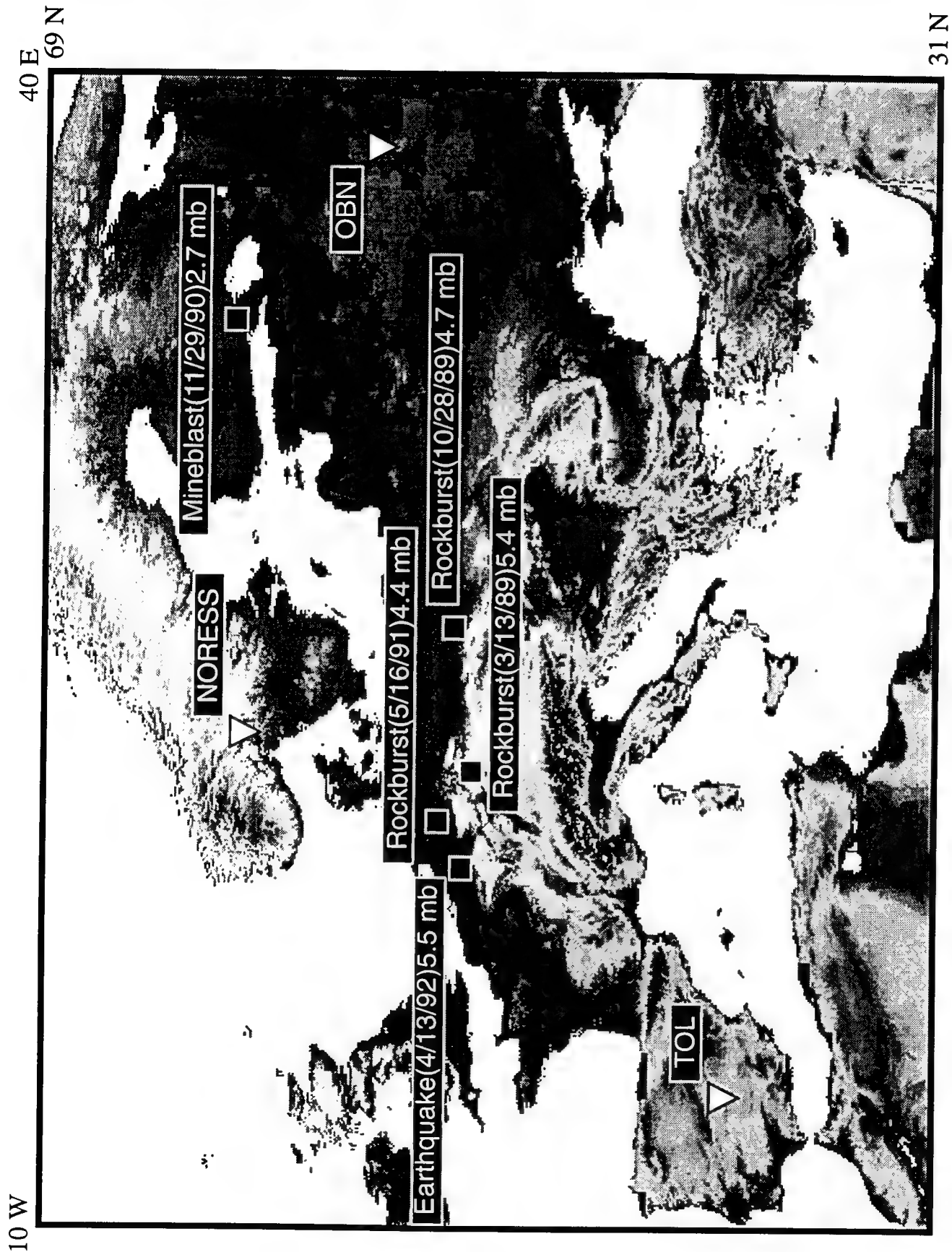
Figure 5. Locations of several rockbursts, an earthquake, and a mineblast in Central Europe used in discrimination analysis. Inverted triangles show selected far-regional stations.
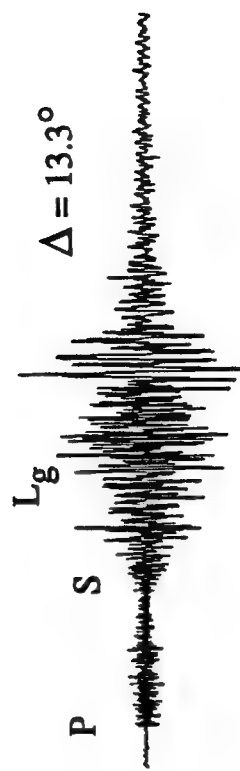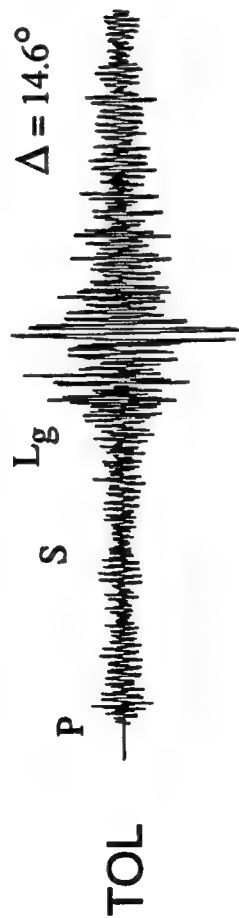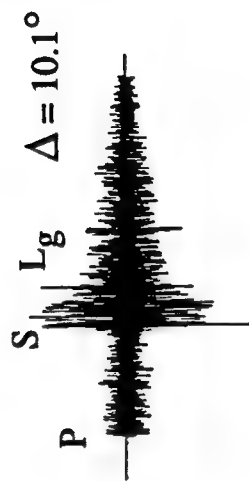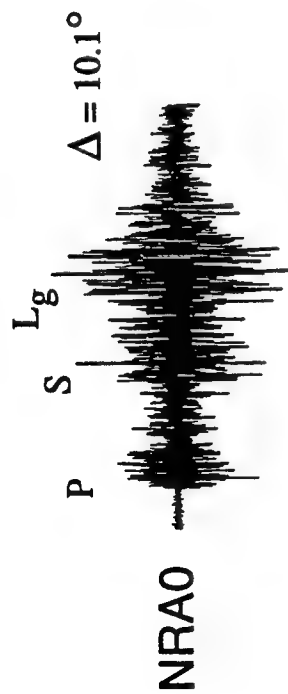
Figure 6. Comparison of vertical-component waveforms at three regional stations from the 1989 German rockburst and the 1992 German/Netherlands border earthquake.

27

the L_g and P signals appear enhanced relative to S for the rockburst on these broader-band recordings. At OBN and TOL S appears somewhat more prominent for the earthquake than for the rockburst, but there is also a very sharp P phase in the earthquake record at OBN. At both OBN and TOL there is evidence of significant long-period surface-wave excitation for both events.

We performed a band-pass filter analysis of the NORESS records for the earthquake and the three rockbursts from Figure 5. Each record was passed through a set of overlapping band-pass filters with similar characteristics but different cut-off frequencies. Comparing the 1989 German rockburst and the 1992 Netherlands earthquake in Figure 7, there is an apparent enhancement of P and L_g relative to S in the rockburst compared to the earthquake which persists at all frequencies. There also appears to be a tendency in the rockburst P to be more prominent relative to other phases at high frequencies. This appears to be contrary to our teleseismic observations which indicated more high-frequency energy in the earthquake P than in the rockburst P for these same events, but the prominence of P here may be related more to a more rapid decline in S and other phases for the rockburst than to actual P enhancement. Spectral analyses of the regional P signals for these events is discussed in greater detail later in this section. The same band-pass filter analyses of the other two rockbursts are shown in Figure 8. In these examples we do not see the strong L_g relative to S 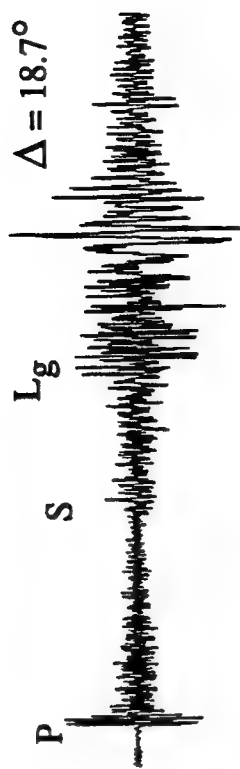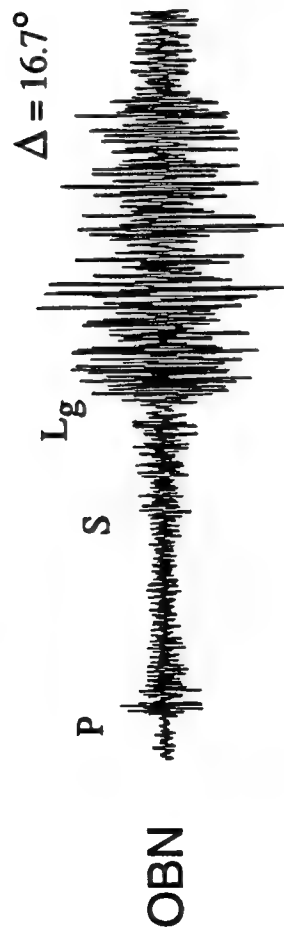at all frequencies; only in the 1989 Polish rockburst is the L_g prominent and primarily at lower frequencies. However, the P signals in these rockbursts again appear to be stronger relative to S than they were for the earthquake in Figure 7. Once again there is a tendency for the rockburst P to increase in prominence at high frequencies relative to other phases.

28
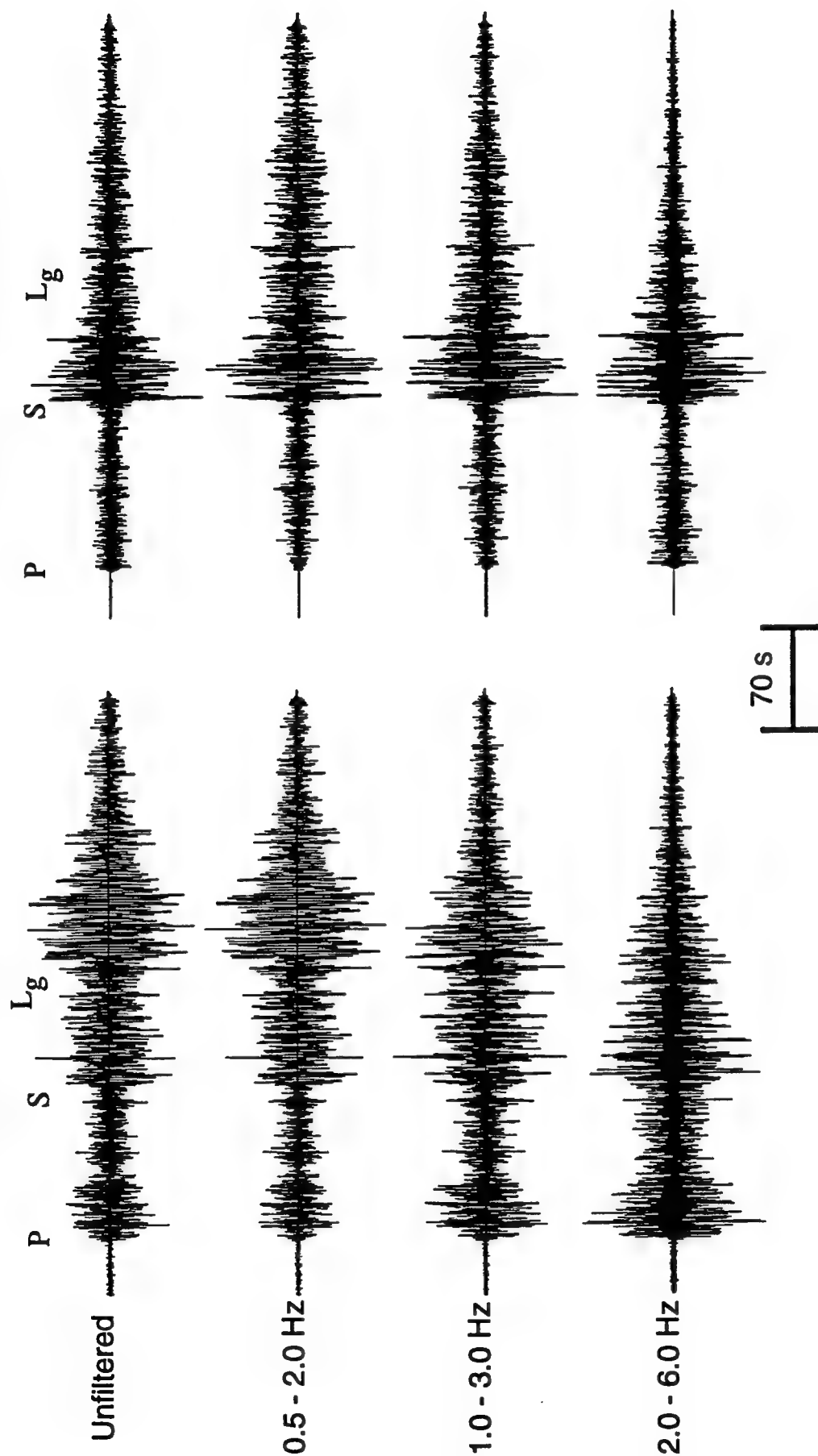
Figure 7. Comparison of band-pass filter analysis of NORESS vertical-component waveforms from the 1989 German rockburst and 1992 German/Netherlands border earthquake.

NORESS

1991 GERMAN ROCKBURST

1989 POLISH ROCKBURST
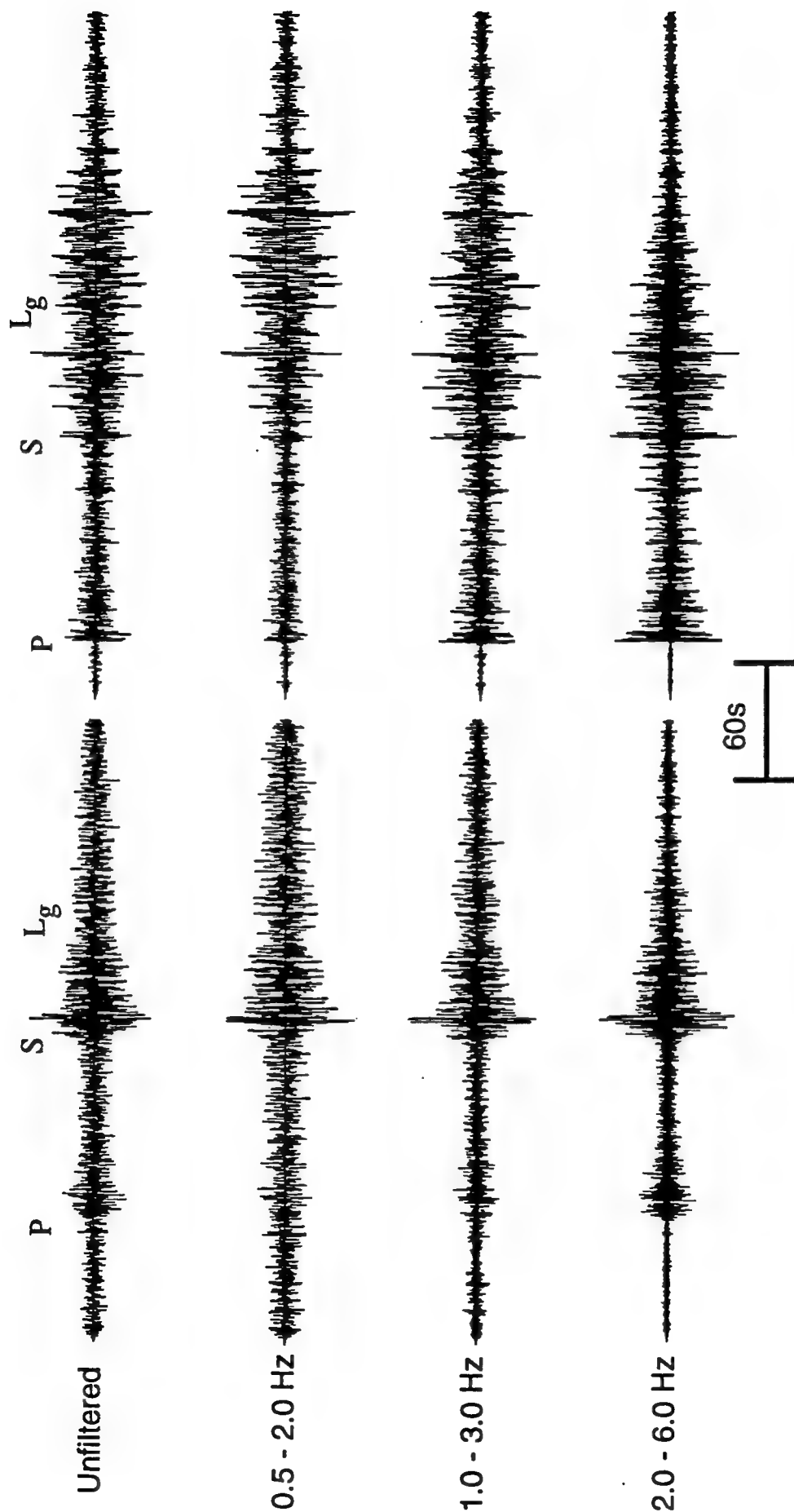
Figure 8. Comparison of band-pass filter analysis of NORESS vertical-component waveforms from the 1991 German rockburst and 1989 Polish rockburst.

30

Figure 9 presents the results from Figures 7 and 8 in terms of parametric measurements of the peak S/P amplitude ratios in each frequency band. The S/P ratios for the 1992 Netherlands earthquake are in the 3 - 5 range declining only slightly with frequency. S/P ratios for the rockbursts are generally in the 1 - 3 range and show more decline with frequency. Similar analyses including a few additional events from the database continued to suggest a tendency for the rockbursts and earthquakes from Central Europe recorded at NORESS to separate on the basis of S/P ratio. However, it should be noted that all events used in these analyses do not have the same propagation path to NORESS; and we have not attempted here to adjust for propagation differences. This is left to future refinement of the method.

3.4 Further Investigation of Far-Regional P Spectra

To better understand the behavior of the far-regional P-wave spectra observed at NORESS, we analyzed the signals from the 3/13/89 German rockburst and the 4/13/92 Netherlands earthquake already described plus the 10/28/89 Polish rockburst (4.7 m_b) and a mineblast near the Russian/Finnish border (11/29/90, 2.7 M_L) as shown in Figure 5 above. All four events are located at comparable epicentral distances from NORESS - 1120 km, 1135 km, 1055 km, and 950 km respectively. All four events produced good P signals at NORESS. Signal levels were well above noise out to frequencies of 10 Hz or more, although the P signal for the smaller magnitude mineblast appears to be contaminated by noise at low frequencies (f < 2 Hz).

We analyzed the spectral behavior in terms of P/P spectral ratios which are shown in Figure 10. For the 3/13/89 rockburst/4/13/92 earthquake

31
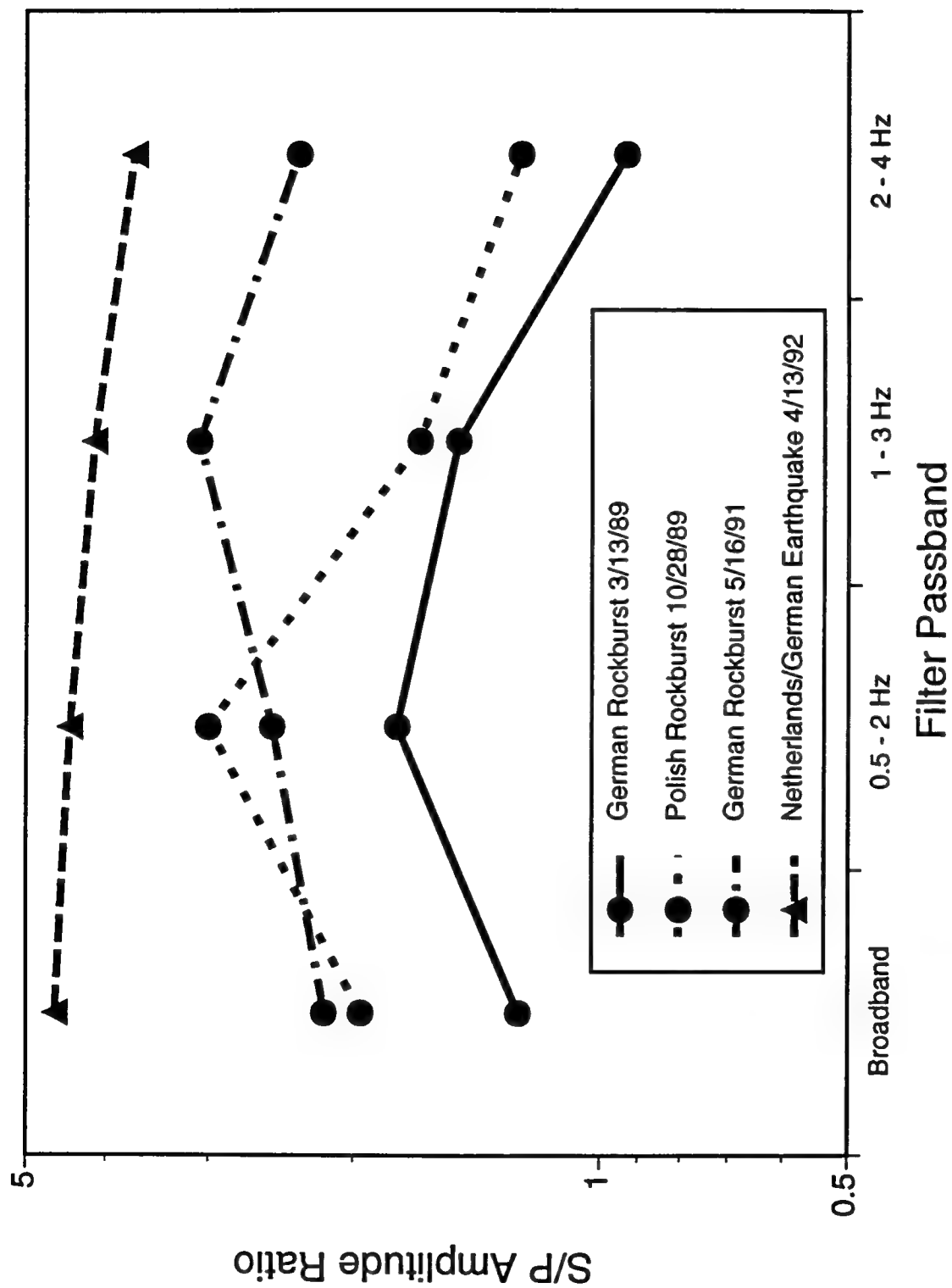
Figure 9. Comparison of S/P ratios at NORESS for various filter passbands for selected Central European rockbursts and Netherlands/German border earthquake.
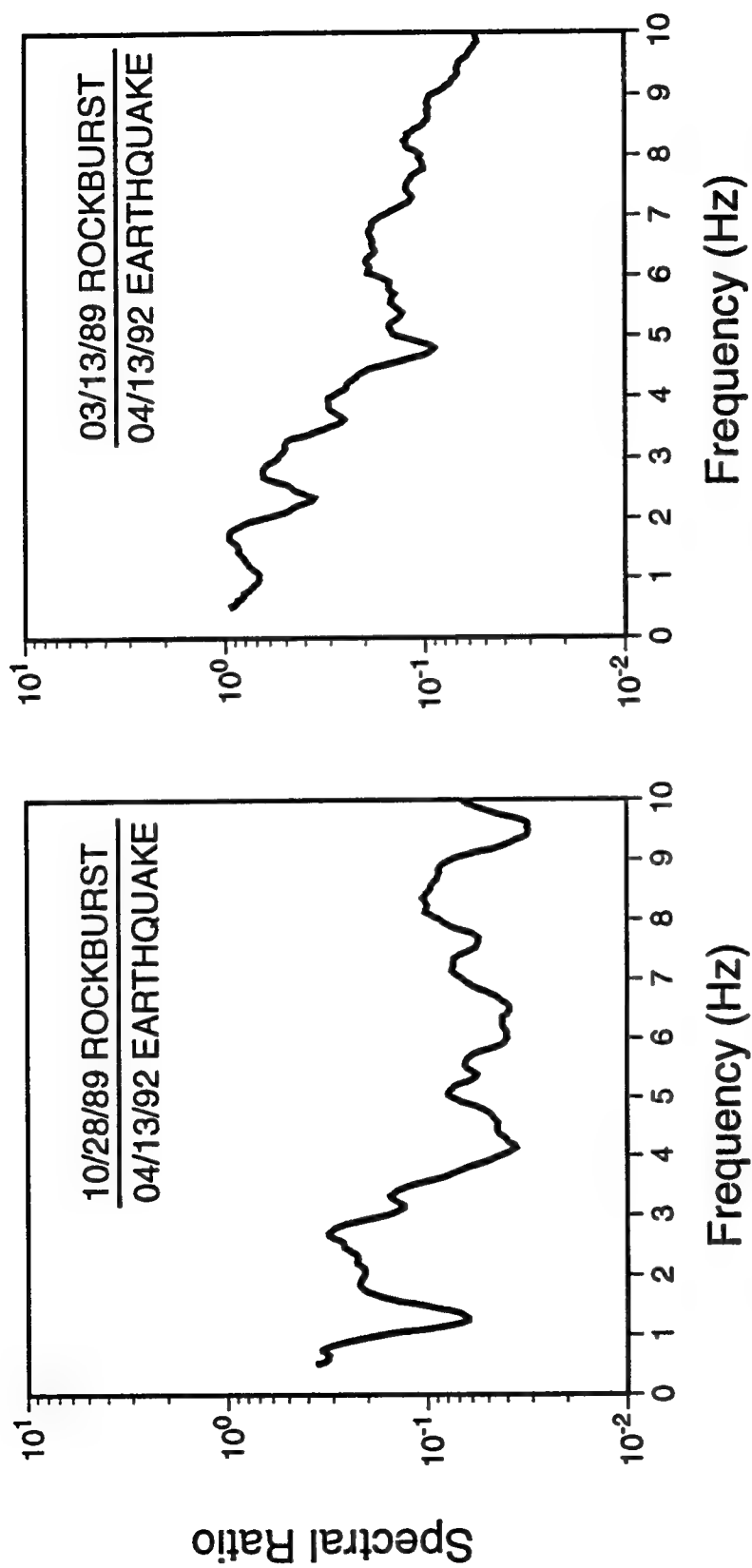
Figure 10. P/P spectral ratios determined from far-regional signals at NORESS for large Central European rockbursts and the large Netherlands earthquake.

comparison, the P/P ratio is near a value of one in the vicinity of 1 Hz. This is consistent with the similar magnitude levels of the two events and with our teleseismic results presented earlier in Section 3.2. The ratio has a peak near 2 Hz, again consistent with the teleseismic results, but generally falls off rather steadily to a value less than 0.1 at 10 Hz. The P/P ratio for the 10/28/89 rockburst/4/13/92 earthquake is somewhat less well-behaved; the ratio shows some spectral holes which produce rapid fluctuations in level. The ratio is well below 1.0 near 1 Hz indicative of the smaller magnitude of the Polish rockburst relative to the earthquake. The P/P spectral ratio tends to decrease with frequency out to about 5 Hz and then levels off up to 10 Hz. Reasons for the leveling off of the ratio are not clear but could be caused by noise contamination or a shift in corner frequency for the smaller event or also possibly by attenuation differences between the two propagation paths.

As another check on the far-regional P signal behavior, we looked at the signals from the 3/13/89 German rockburst and the 4/13/92 Netherlands earthquake recorded at the AEDS station in Sonseca, Spain. The epicentral distances in this case were 1310 km and 1285 km from the German rockburst and the earthquake respectively. The S/N comparisons for the earthquake indicate good, strong signals which are well above noise over a broad band from low frequency out to beyond 5 Hz. However, for the rockburst the signal is unusually low, approaching noise near 3 - 5 Hz. We, nevertheless, computed the P/P spectral ratio over the band from 0.5 to 5 Hz as shown in Figure 11. The ratio is generally very low (less than 0.1) over most of the band and shows a tendency to decline with increasing frequency. We assume there is some problem in the calibration information provided for the Sonseca station for the

34
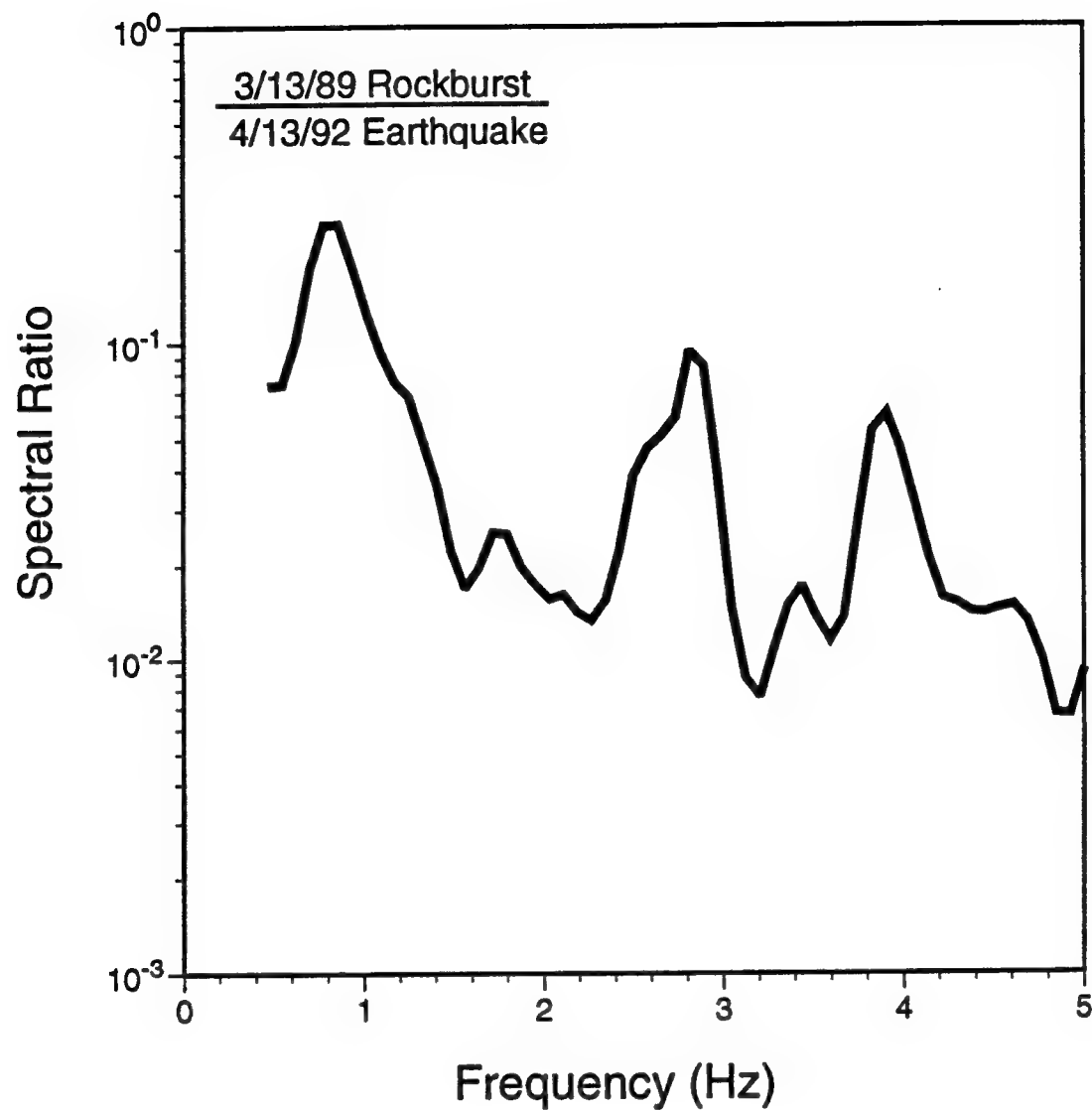
Figure 11. P/P spectral ratio determined from far-regional signals at the Sonseca, Spain AEDS station for the large Central European rockburst and earthquake.

3/13/89 rockburst waveforms. This assumption appears to be supported by observations of these same two events on the nearby GDSN station at TOL, where the amplitude difference between the two events is seen to be only about 30 percent. Disregarding the difference in level, the trend in the ratio in Figure 11 again would indicate a more rapid decline in high-frequency energy in the 3/13/89 rockburst than in the 4/13/92 earthquake.

For the 11/29/90 mineblast/4/13/92 earthquake comparison the P/P spectral ratio is presented in Figure 12. We see that the ratio has a low value much less than 0.1 - near 1 - 2 Hz in keeping with the much lower magnitude of the mineblast compared to the earthquake. However, the ratio shows a tendency to increase with frequency out to 10 Hz. The behavior might represent some combination of the excitation mechanism and corner frequency. Scaling analyses would be useful to identify to what extent the higher corner frequency of the smaller magnitude event (viz. mineblast) influences the spectral ratio. Higher frequencies in the mineblast might also be attributed to propagation path differences if it can be assumed that the path from NORESS into Finland has lower P-wave attenuation than the path to the south into Europe and the Netherlands.

We would conclude from these observations that the far-regional P-wave observations for Central Europe are generally consistent with the teleseismic P-wave observations reported above. Both teleseismic and far-regional P waves for the 3/13/89 rockburst appear to have less high frequency energy than similar P waves for the 4/13/92 earthquake. However, interpretation of the behavior for the other events is more problematic. The Polish rockburst (10/28/89), for which we analyzed the far-regional P signals, appears to have less high-frequency
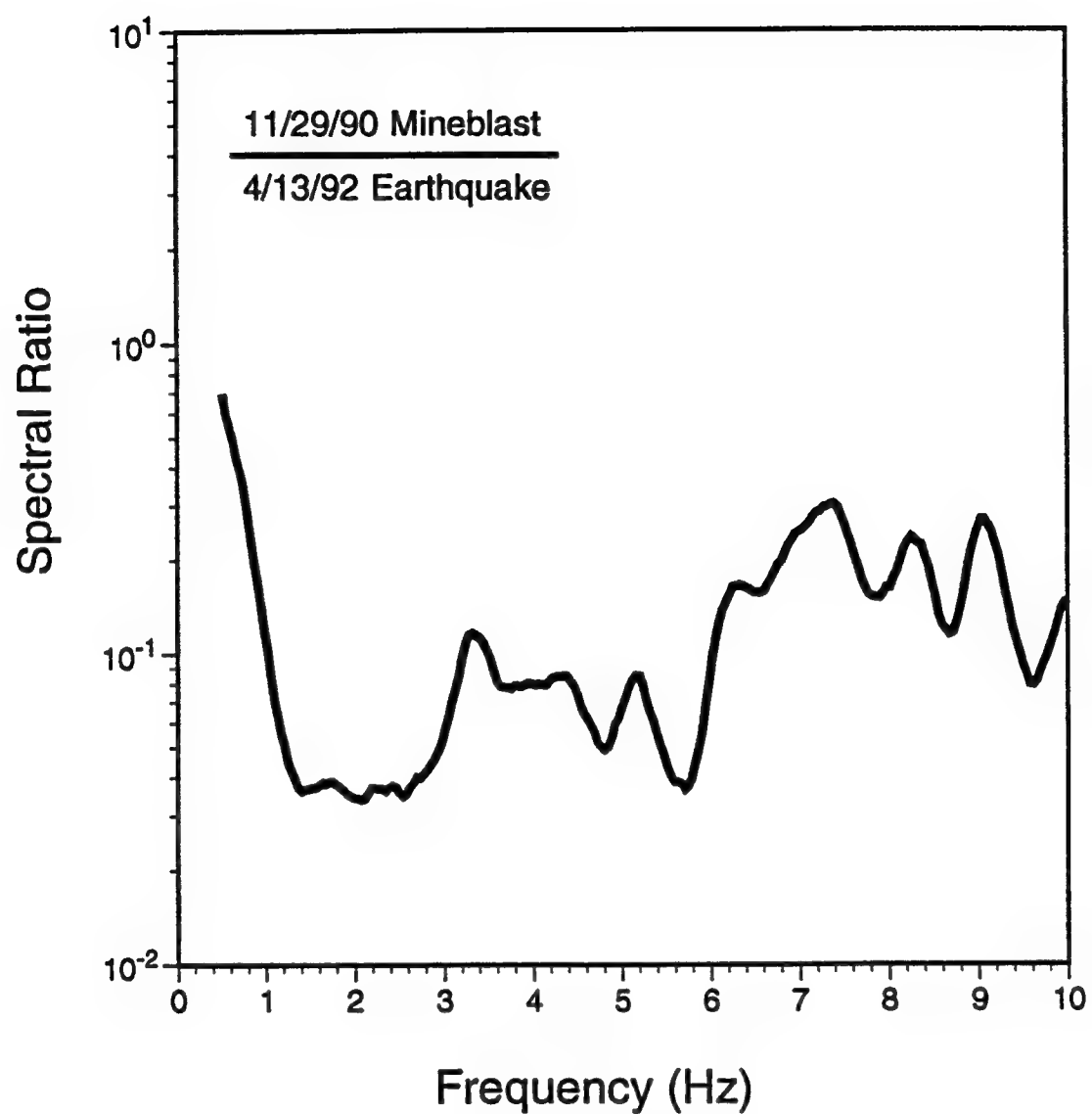
Figure 12. P/P spectral ratio determined from far-regional signals at NORESS for a mineblast near the Finnish/Russian border and a large Central European earthquake.

energy than the earthquake; while the Polish rockburst (6/29/89), for which we analyzed teleseismic P, shows the opposite trend. A reasonable interpretation of the results appears to be that rockburst or mine tremor mechanisms may vary in the efficiency with which they excite P-wave energy in different frequency bands. Theoretical model studies and improved knowledge of path attenuation effects could provide important evidence to test this hypothesis.

3.5 Nearer-Regional Observations ·

Our final analyses of the Central European events focuses on nearer-regional observations at station GRFO. In these analyses we primarily relied on data from three events: the 8/15/81 Polish rockburst (4.0 M_L), the 4/14/92 aftershock (4.3 M_L) of the Netherlands earthquake, and the 11/02/92 Swiss munitions blast (4.0 M_L). As noted, the events all had roughly the same magnitudes; and, as can be seen in the map in Figure 13, they are each located at about the same epicentral distance from GRFO (390 km, 387 km, and 393 km respectively).

Figure 14 shows the vertical component records for the three events. Approximate times of P_n, P_g, and L_g phases are identified on the records. The L_g phases are the largest on the broadband recordings for all three events. S phases, expected at the beginning or just prior to the L_g window, are not separated or distinct on the records. The P_g phases are most strongly excited for the Swiss munitions blast and Polish rockburst, and P_n is strongest for the rockburst. The events all produce quite similar maximum amplitude levels at GRFO. Fourier spectral analyses were performed on the time segments corresponding to each of the identifiable regional phases for each event, as

38
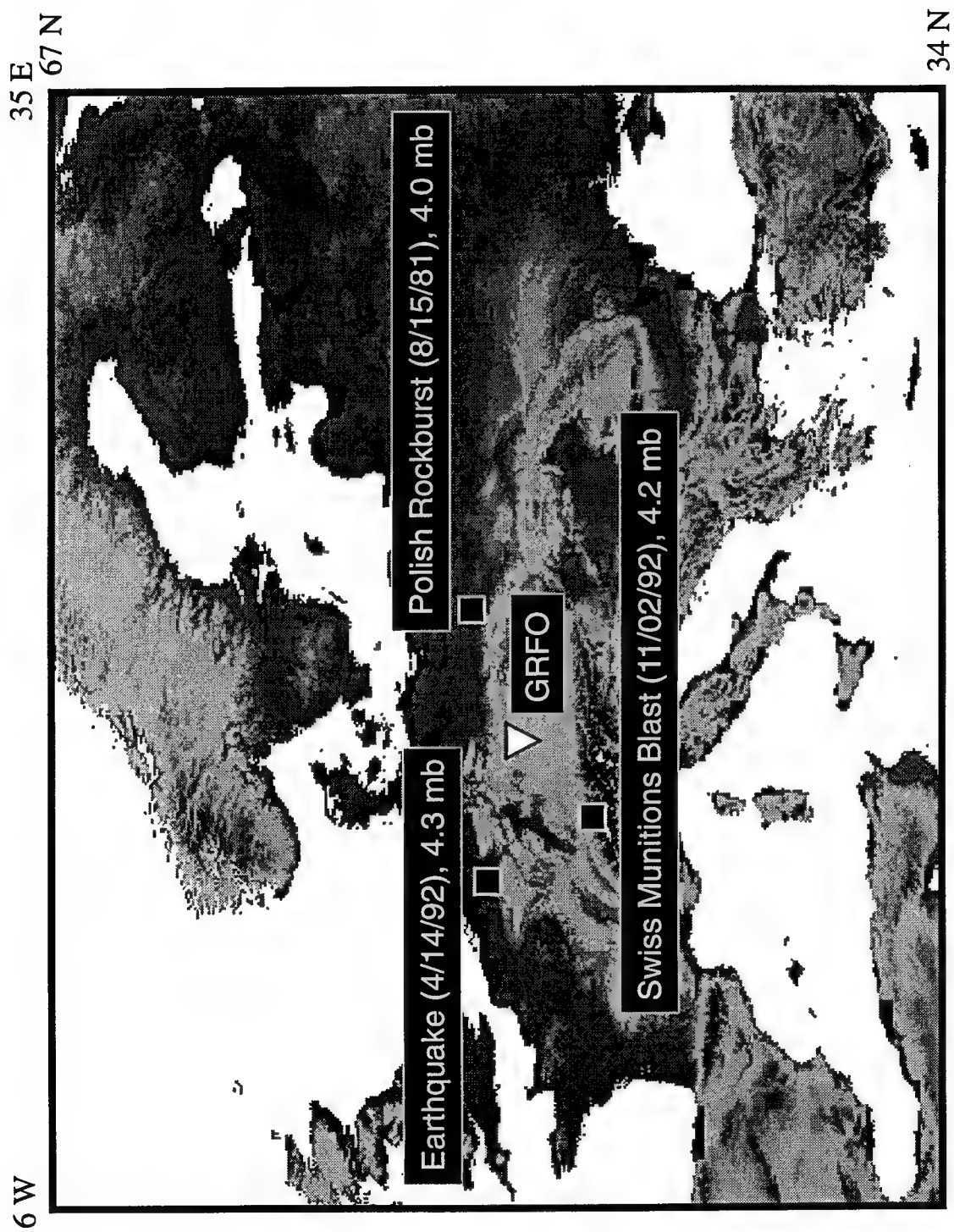
Figure 13. Locations of three different source types used in discrimination analyses for station GRFO.

39
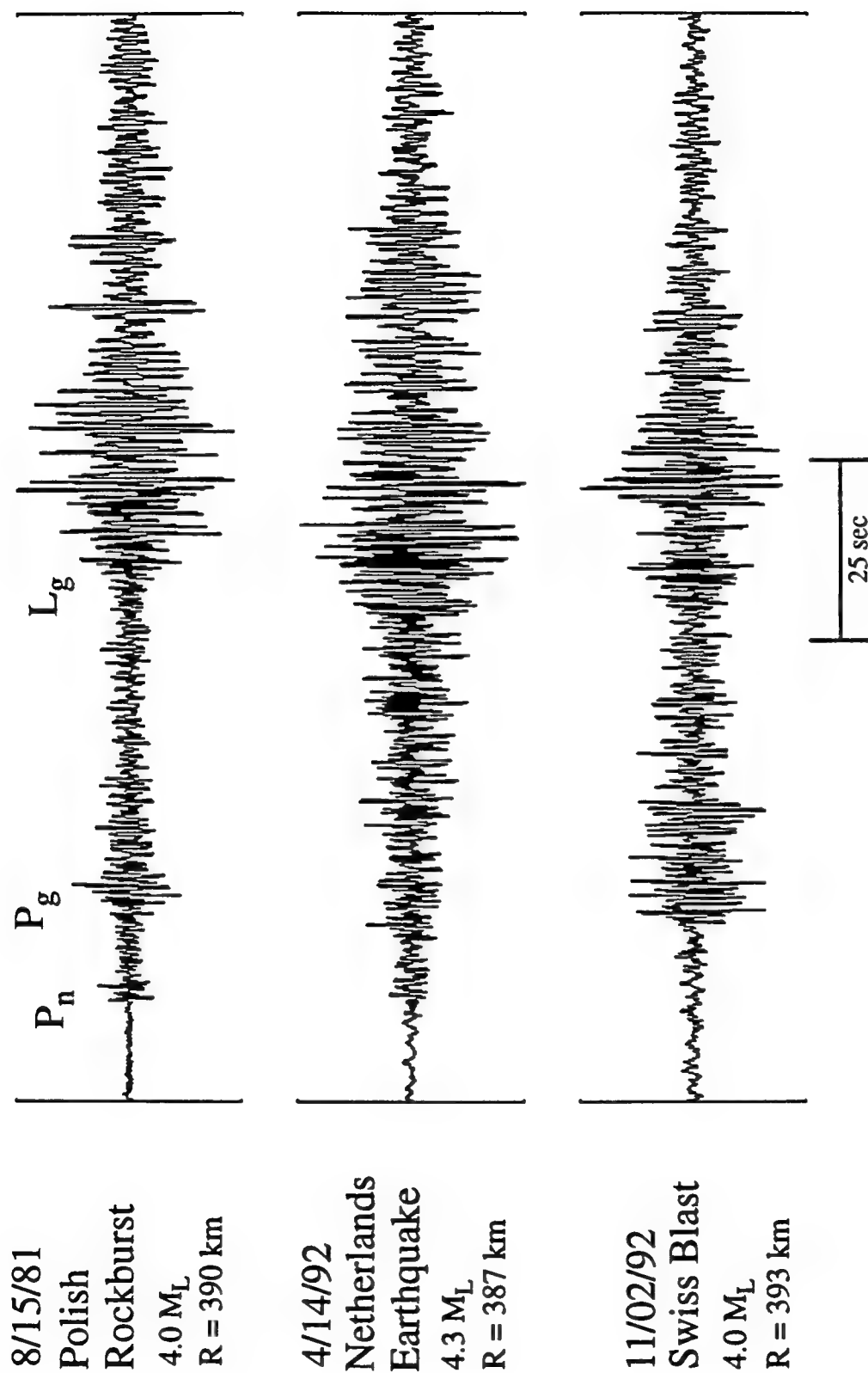
Figure 14. Vertical-component records at GRFO from three different source types.

P_n

P_g

L_g

25 sec

8/15/81
Polish
Rockburst

4.0 M_L
R = 390 km

4/14/92
Netherlands
Earthquake

4.3 M_L
R = 387 km

11/02/92
Swiss Blast

4.0 M_L
R = 393 km

40

well as for noise segments preceding the P_n signals for each. Window segments used in these analyses were generally 12.5 seconds in duration except in one or two cases where shorter segments were used to avoid some minor data glitches which contaminated the records for parts of the regional phase windows. Figure 15 shows signal and noise spectra for each of the regional phases as determined from the GRFO recording of the 8/15/81 Polish rockburst and is typical of the spectra for all the events. The S/N levels are generally good to somewhere in the 6 - 8 Hz range; S/N levels are lowest for the P_n phases. Even though the S/N is much greater than 1.0, earthquake spectra tend to flatten out above 6 Hz which might be indicative of some type of noise problem at higher frequency.

Previous studies of regional seismic discrimination (cf. Bennett et al., 1992) have demonstrated the potential merits of comparing relative excitation of different regional phases for use in identifying source types. We, therefore, decided to compute the spectral ratios of the individual regional phases to one another - i.e. L_g/P_n and L_g/P_g. We show here the L_g/P_g ratios because of the better S/N conditions for P_g and consequent lower danger of noise contamination in the ratios. These ratios for the three events recorded at GRFO are plotted in Figure 16 for the band 0.5 - 6 Hz in which S/N is generally well above one for the individual phases. The L_g/P_g ratio for the rockburst tends to be highly oscillatory with frequency but maintains an overall level just below a value of 2 with no particular evidence of increase or decrease with increasing frequency. The L_g/P_n spectral ratio for this event produced quite similar behavior to the L_g/P_g ratio. L_g/P_g for the earthquake tends to be less oscillatory about a value near 3 and may increase slightly toward higher frequencies. The

41
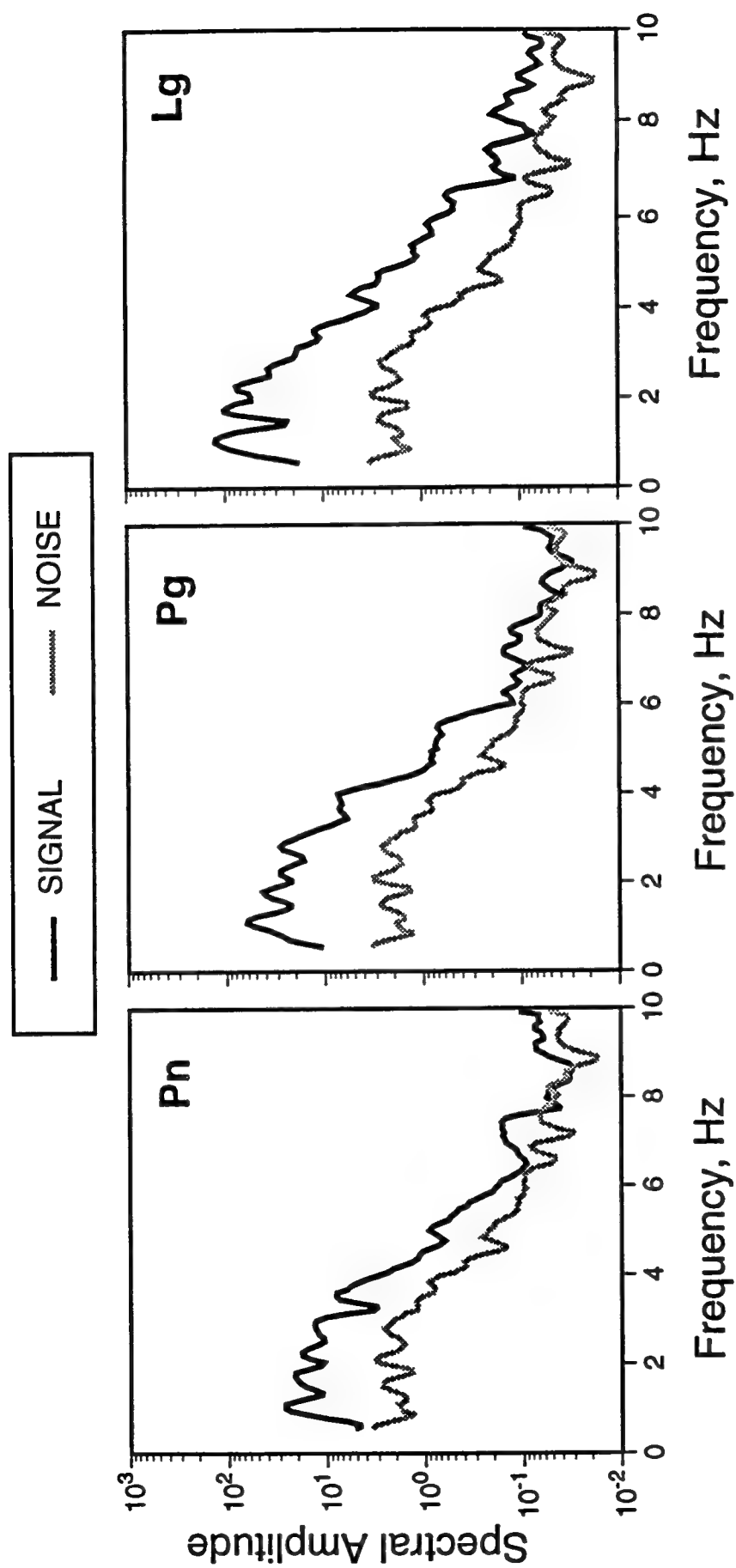
Figure 15. Example of signal and noise spectra for the regional phases recorded on the vertical component at GRFO from the 8/15/81 Polish rockburst.
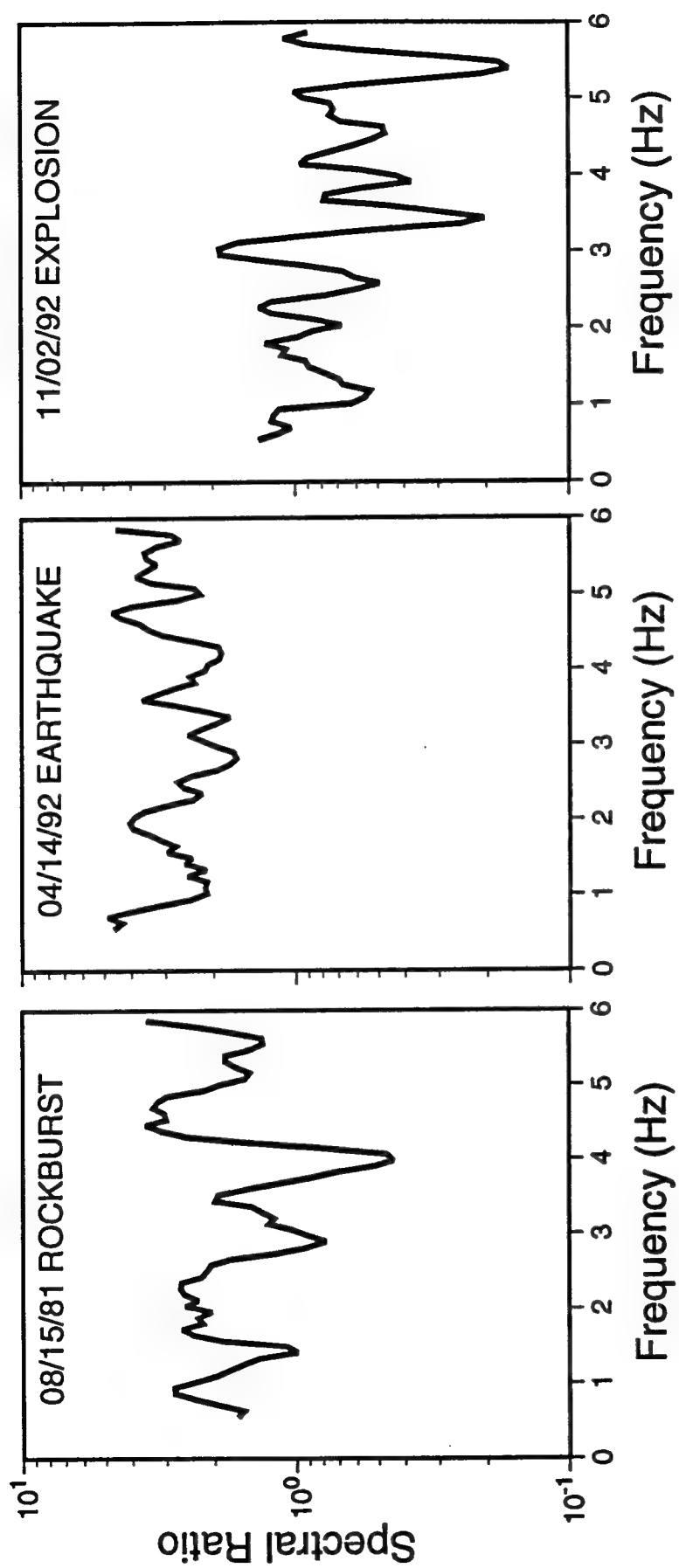
Figure 16. Lg/Pg spectral ratios determined at GRFO for the three different source types.

43

L_g/P_n ratio for the earthquake was somewhat more oscillatory and showed a stronger tendency to increase with frequency. L_g/P_g for the Swiss blast is again highly oscillatory but maintains a much lower level near 0.7. There is also a tendency in the ratio to decrease with frequency, which again appears to show up more strongly in the L_g/P_n ratio for the blast.

In Figures 17 and 18 we compare the individual phase spectra, P_g and L_g, observed at GRFO for the events. For the 8/15/81 rockburst and the 4/14/92 earthquake in Figure 17, the P_g spectra appear generally similar in level and shape; although the earthquake shows a slight, but definite, tendency to have more higher frequency energy. The L_g spectrum for the rockburst has a similar level to the earthquake in the 1 - 2 Hz band but drops off much more rapidly at high frequencies than the corresponding earthquake spectrum. In Figure 18 the P_g spectrum for the Swiss blast is strongly enriched (by a factor of about 3) in the band 1 - 2.5 Hz and slightly enhanced in the band 4.5 - 6 Hz compared to the earthquake. The L_g spectrum for the Swiss blast and the earthquake nearly coincide up to about 3 Hz, but above 3 Hz the blast L_g spectrum drops off abruptly to a level 3 or more below the earthquake. Propagation differences related to the different paths into GRFO for these three events might contribute to the variations in spectral behavior, but source mechanism differences might also be a cause. Additional investigations of regional propagation effects for this area and theoretical modelling of the source effects could help resolve which factors are significant.

The behavior at GRFO of the P/P spectral ratios between different event types is illustrated in Figure 19 for P_g phases. The rockburst to earthquake ratio shows a clear and steady decrease with frequency. This observation appears
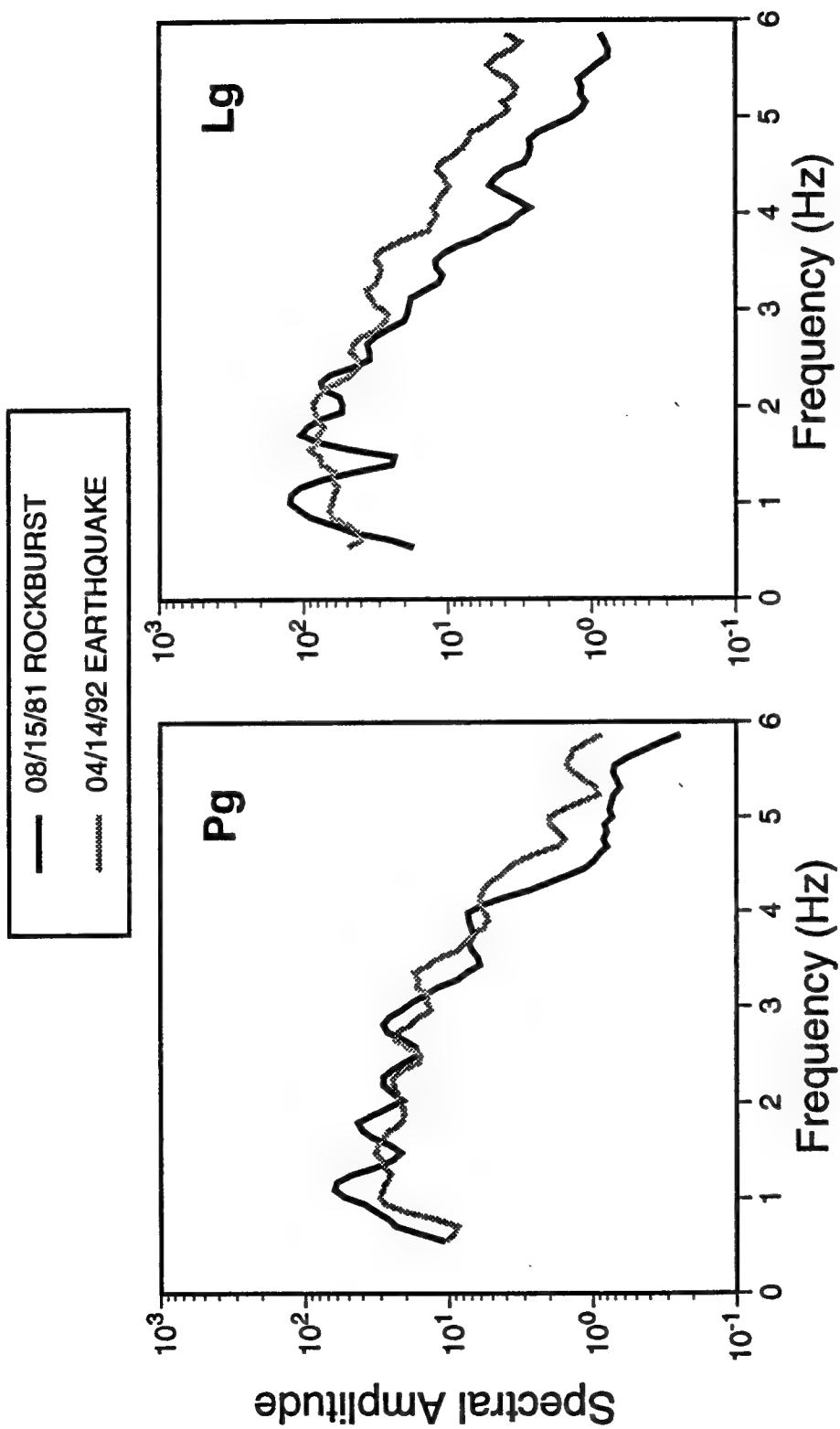
Figure 17. Comparison of Pg spectra and Lg spectra determined at GRFO for the rockburst and earthquake from Figure 13.
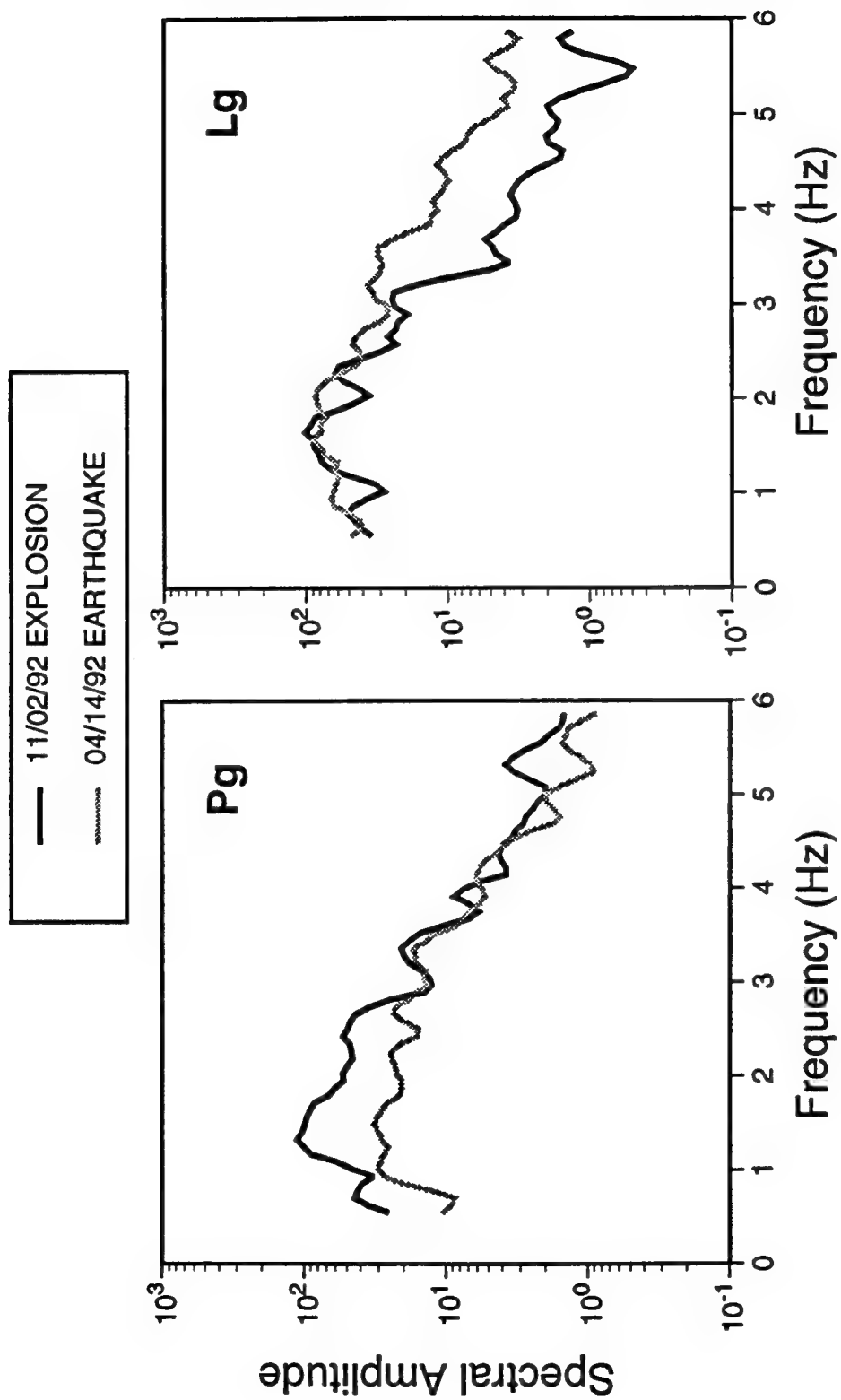
Figure 18. Comparison of Pg spectra and Lg spectra determined at GRFO for the explosion and earthquake from Figure 13.
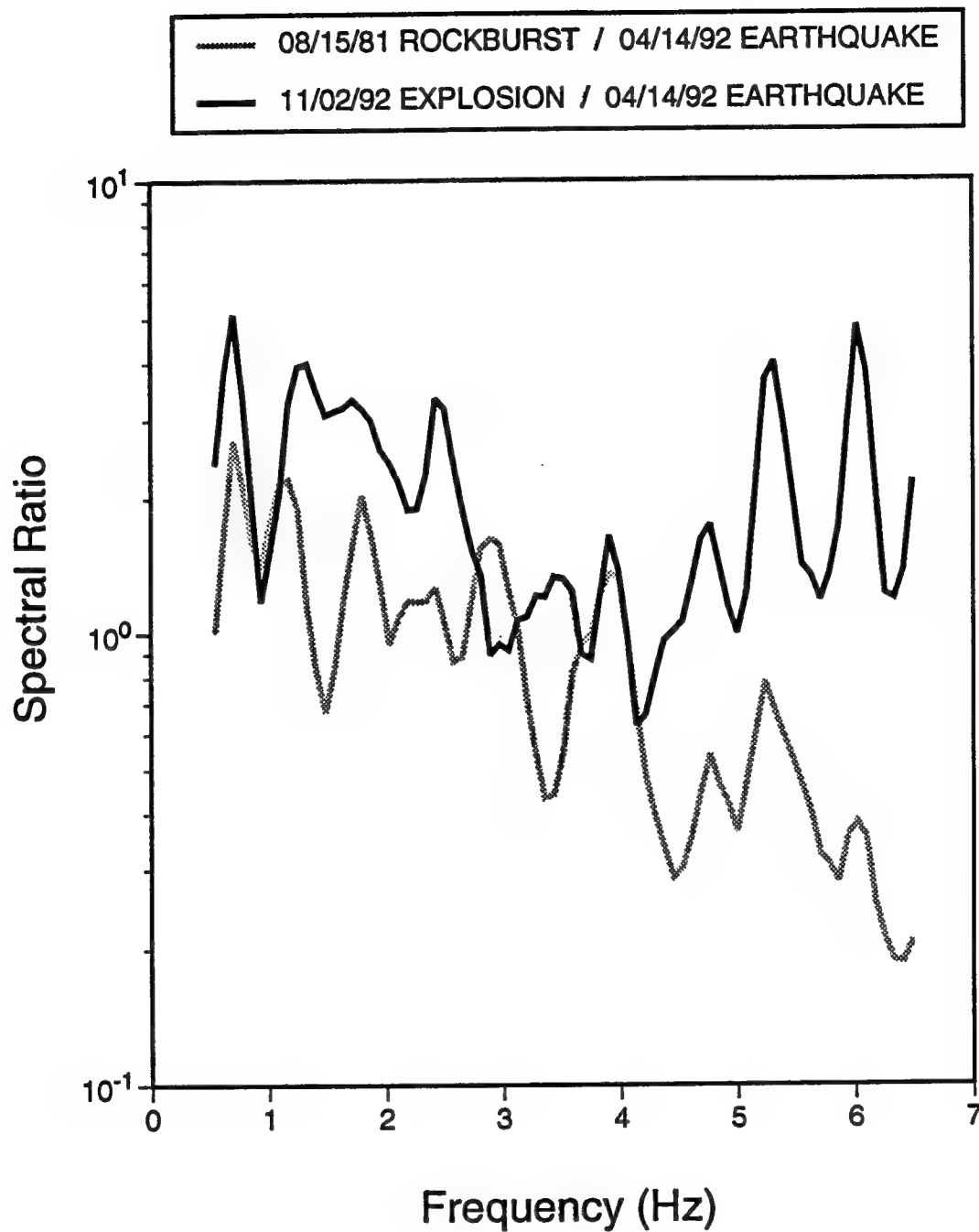
Figure 19. Comparison of P/P spectral ratios determined at GRFO from the different event types from Figure 13.

to be consistent with our previous observations reported above for teleseismic P and for far-regional P from German and some Polish rockbursts relative to earthquakes. The behavior of the P_g/P_g spectral ratio for the 11/02/92 explosion/4/14/92 earthquake is more complex. After a slow decrease with frequency to near 4 Hz, there appears to be a slight increase toward higher frequencies. The Pn/Pn spectral ratios, not shown, exhibit a steady decrease with frequency over the entire band for the rockburst/earthquake ratio; while the blast/earthquake ratio show a gradual increase with frequency over the available frequency band. These latter results suggest the possibility of some discrimination capability between different source types in the regional phase spectra, but additional studies are needed to resolve propagation path influences and demonstrate the capability for larger samples of events.

4. South African Rockbursts

4.1 Teleseismic Signals

As noted above, many large rockbursts occur in the gold-mining region of South Africa. While these large events ($M_L \approx 5$) frequently produce good signals at teleseismic stations throughout much of the world, there is little natural earthquake activity or man-made explosions of similar size from this source region which can be used to provide comparisons for use in discrimination studies. Figure 20 shows a comparison of vertical-component records at three teleseismic AEDS stations for a large South African rockburst (10/28/86, 5.2 m_b) and the largest presumed earthquake (9/05/83, 4.7 m_b) from our database. As can be seen by comparison to other events in Table 2 above, this earthquake was located considerably south and west of the primary rockburst zone. There also appear to have been some aftershocks, including one within about seven seconds after the main event, reported in the NEIC catalog. These observations tend to corroborate the identification of the event as an earthquake.

Comparing the signals the P waveform for the rockburst appears to be significantly more complex than that of the earthquake. The rockburst P appears to include several oscillations which could be attributed to multiplicity in the source or possibly reverberation in the source crust. On the other hand, the earthquake P seems to be a rather simple pulse (particularly noticeable at the BC station). This behavior is similar to that described in Section 3.1 above for the signals from Central European earthquakes and rockbursts at teleseismic stations. The second pulse, arriving about 7 seconds after the initial

49
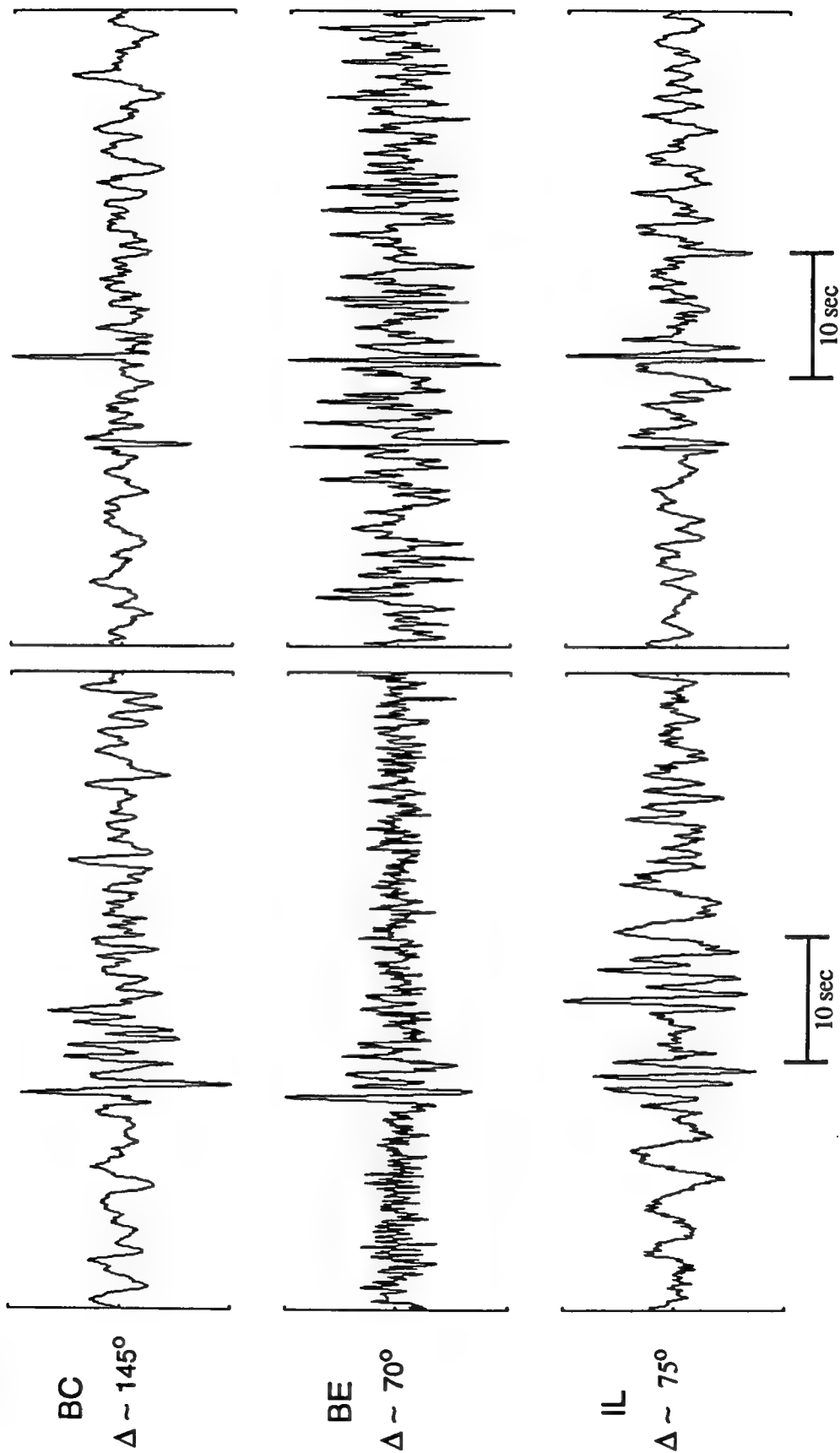
Figure 20. Comparison of vertical-component, teleseismic P signals at three AEDS stations from a large South African rockburst and a nearby presumed earthquake.

P in the earthquake record, has been identified as P from an aftershock, according to the NEIC interpretation. If the event is indeed an aftershock, it appears that the mechanism must be substantially different - in particular, the pulse polarity seems to be reversed at station BC and possibly at the other stations. The limited waveform data that we have looked at here might support an alternate interpretation of the second pulse as a depth phase. If the phase is pP, the focal depth for the earthquake corresponding to the 7-second delay is about 20 km. We do not know, at this time, whether other observations, including regional data, would permit this alternative interpretation. Nevertheless, following either interpretation appears to support the conclusion that the main event was an earthquake.

4.2 Spectral Comparisons of Teleseismic P

In addition to simple waveform comparisons, we have performed spectral analyses of the teleseismic P signals recorded at the AEDS stations for several South African events. These analyses were similar to those performed on the AEDS teleseismic signals for Central European events as described in Section 3.2 above. Many of the teleseismic AEDS stations are at very large epicentral distances from South African events ($65^\circ < \Delta < 145^\circ$). As a result, many of the P signals from South African events have experienced greater attenuation, and the useful frequency band of the spectra is more limited. In addition, while the signal at the nearer is the normal teleseismic P, the signal at the more distant stations is PKP. Since our analyses utilize spectral ratios between nearby events at the same station, whether we are using P/P or PKP/PKP ratios should not be significant to our interpretation. We have analyzed the signals from three

51

of the largest South African rockbursts in our database: 1/25/89, 5.5 m$_b$; 9/26/90, 5.4 m$_b$; and 11/03/91, 5.1 m$_b$. Nine common stations were selected for the first two events, and six for the latter two events.

Fourier spectra for 7.5-second P-wave segments and similar noise segments were calculated, and signal versus noise analyzed as a function of frequency. At some stations signals were only above noise out to about 3 Hz. P/P spectral ratios were computed using the common-station signal spectra pairs for 1/25/89/9/26/90 and 11/03/91/9/26/90. The spectral band in which S/N ratios were generally greater than one was again used to limit the stations contributing to an average ratio which was computed for each event pair. The average ratios with plus- and minus-one-sigma bounds about the mean are shown in Figure 21. In both cases the average P/P ratios show some fluctuations with frequency, but the fluctuation about the overall trends are not too great. For the 1/25/89/9/26/90 ratio, the ratio oscillates about a level somewhat above 1.0. There also appears to be a slight decrease in the average ratio with increasing frequency from a value near 2 at 1 Hz to a value near 1 at 4.5 Hz. For the 11/03/91/9/26/90 P/P spectral ratio, the fluctuations are somewhat less regular. The level of the ratio is generally below one over much of the band and shows a tendency to increase with frequency from a value near 0.5 at 1 Hz to a value near 1.0 at 3.5 Hz. This observation of differences in the frequency content of teleseismic P for rockbursts at nearby source locations appears to corroborate our preliminary observations (cf. Bennett et al., 1993) based on GDSN station measurements.

Several factors may contribute to the observed differences in P-wave spectra and P/P spectral ratios even though the source types are similar. The

52
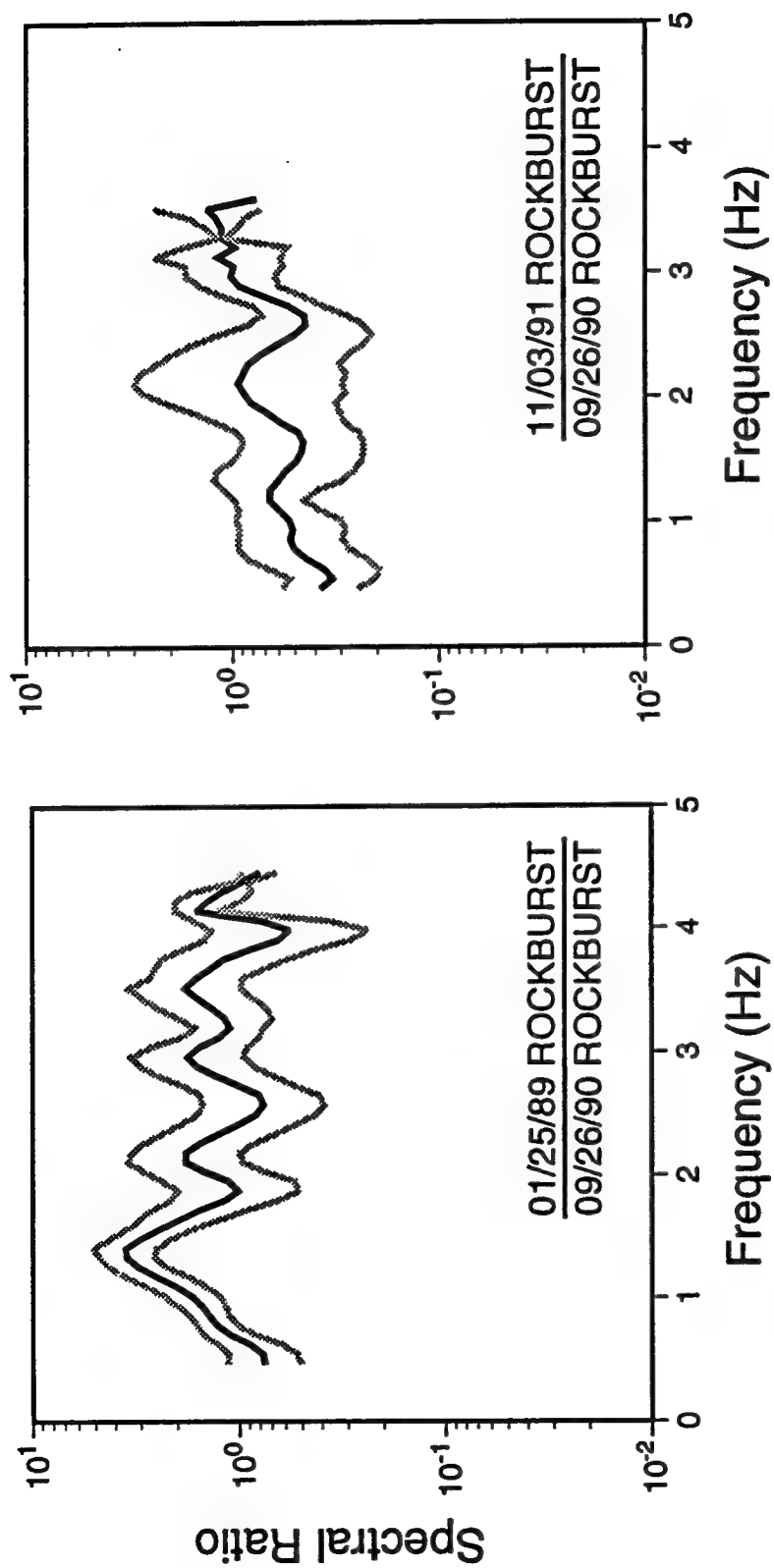
Figure 21. Average P/P spectral ratios and ±1σ bounds determined from teleseismic AEDS stations for large South African rockbursts.

first two South African rockburst events are in roughly the same location (mine) while the third is almost 100 km to the north. It is unclear to what extent source location differences, such as different site response, might cause the observed variations in the two P/P spectral ratios. In addition, the differences in event sizes is not great but might be responsible also for some frequency and level dependence in the ratios. The smaller event would be expected to have a somewhat higher corner frequency, so that the P/P spectral ratio of a smaller event to a large event should be enhanced at higher frequencies. This, in fact, appears to be consistent with our observations in that the increasing ratio in Figure 21 corresponds to the ratio of a smaller to a larger event, while the decreasing ratio in Figure 21 corresponds to the ratio of a larger to smaller event. However, other factors including mechanism variations might also contribute to the observation. For example, events with similar body-wave magnitudes could be expected to produce different P/P spectral ratios because the source time function might be different for a complex roof collapse than for a simple fracture mine tremor. As noted above, well-designed theoretical studies along with some additional analyses of observations could do much to resolve some of the outstanding issues.

With regard to comparisons of teleseismic P spectra between earthquakes and rockbursts in South Africa, we have used the P signals recorded at the three AEDS stations from the two events described above in Section 4.1 (viz. the 10/28/86 rockburst and the 9/05/83 earthquake. The Fourier spectra were computed from a 6-second window of the P-wave (cf. Figure 20 above) which was selected to exclude the P signal of the aftershock (or pP phase) from the main earthquake P segment. We again computed P/P

54

spectral ratios for the rockburst/earthquake and computed an average ratio over those frequencies in which the S/N level was determined to be adequate at each station. This average P/P spectral ratio is shown in Figure 22 over the frequency band from 0.5 to 5 Hz. The ratio is fairly consistent between stations with each showing a relative maximum in the vicinity of 1 Hz and a relative minimum just above 1.5 Hz. The ratio fluctuates somewhat about a level near 3.0 at lower frequencies consistent with the 0.5 magnitude unit difference between the two events. At the higher frequency end, the spectral ratio is lower; but we are less confident in the values there because of noise contamination at some stations. If we accept the lower P/P ratio at high frequencies, the observation here would be consistent with the main results which we reported above in Section III for the Central European rockburst and earthquake comparisons. However, the trends here are not strong, and we would like to have additional corroboration.

4.3 Regional Observations

Our regional signal analyses for South African events is limited to observations from the near-regional DWWSSN station SLR; there are no high-quality stations at far-regional distances for the South African rockburst zone. The distance to SLR from events in the South African rockburst zone is from about 50 km to about 300 km, and most regional earthquakes are located at somewhat greater distances. For a database including 31 mine tremors and 10 regional earthquakes recorded at SLR, Bennett et al. (1993) found that the time-domain measurements of maximum P versus maximum L_g were intermingled. This is illustrated in Figure 23, extracted from that previous report. The L_g/P
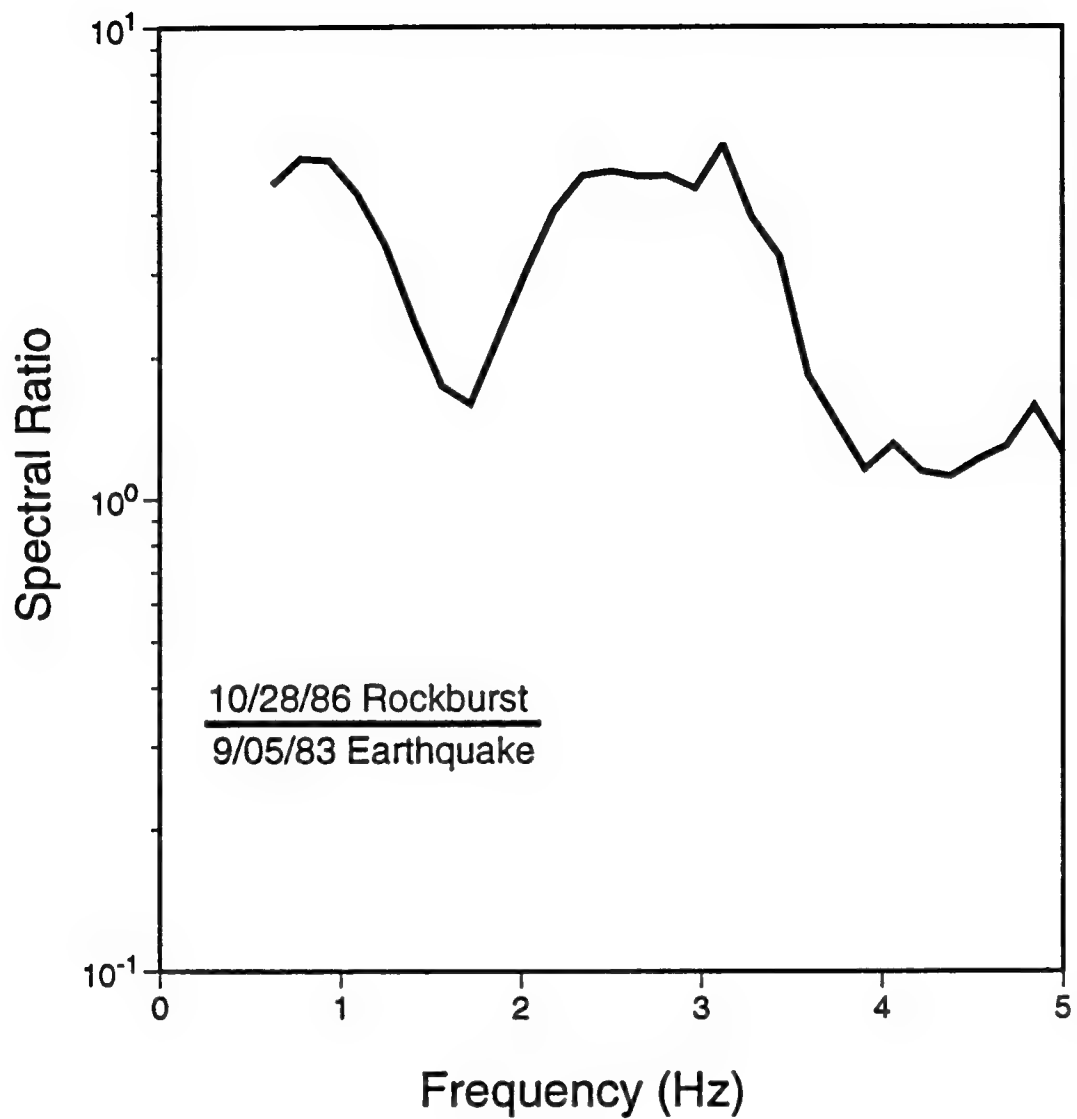
Figure 22. Average P/P spectral ratio determined from three teleseismic AEDS stations for a large South African rockburst and nearby presumed earthquake.

Figure 23. Comparison of the maximum P versus maximum L_g amplitudes measured from time-domain records at SLR from 31 mine tremors and 10 southern Africa earthquakes.

ratios for both the rockburst and earthquakes from South Africa have values well-above one and show no tendency to separate relative to source type. We also showed in the previous report that adjustments for propagation path length did not seem to make much difference in this observation.

In the discussion of the teleseismic P observations above for South Africa, we noted apparent variability between rockburst events from essentially the same source area. Regional observations at station SLR for some of the smaller rockburst events in our database appear to corroborate variability in spectral behavior and mechanism between nearby mine tremors. Figure 24 shows a comparison of the L_g spectra for two mine tremors from the Orange Free State mining area. These two events are located at a range of about 290 km from SLR and are separated from each other by less than 5 km. Considering the uncertainty in epicenter location within the region, the two sources are essentially co-located. The L_g spectra for the two events have somewhat similar shapes. The difference in amplitude level in the frequency band from about 0.5 to 2 Hz amounts to about a factor of three which is just slightly greater than the 0.4 magnitude unit difference between the two events (viz. 3.6 M_L versus 3.2 M_L for the 11/19/81 and 5/24/83 rockbursts respectively). The L_g spectrum for the 11/19/81 rockburst decays more rapidly than that for the 5/24/83 rockburst, and as a result the latter event has relatively more high frequency. This may be partly, but probably not completely, accounted for by the shift in corner frequency toward higher frequencies for the smaller event.

Another observation which appears to support variability in the mechanism of South African rockbursts is the regional P-wave first motions. In Figure 25 we show the expanded first motion plots at station SLR for five

58
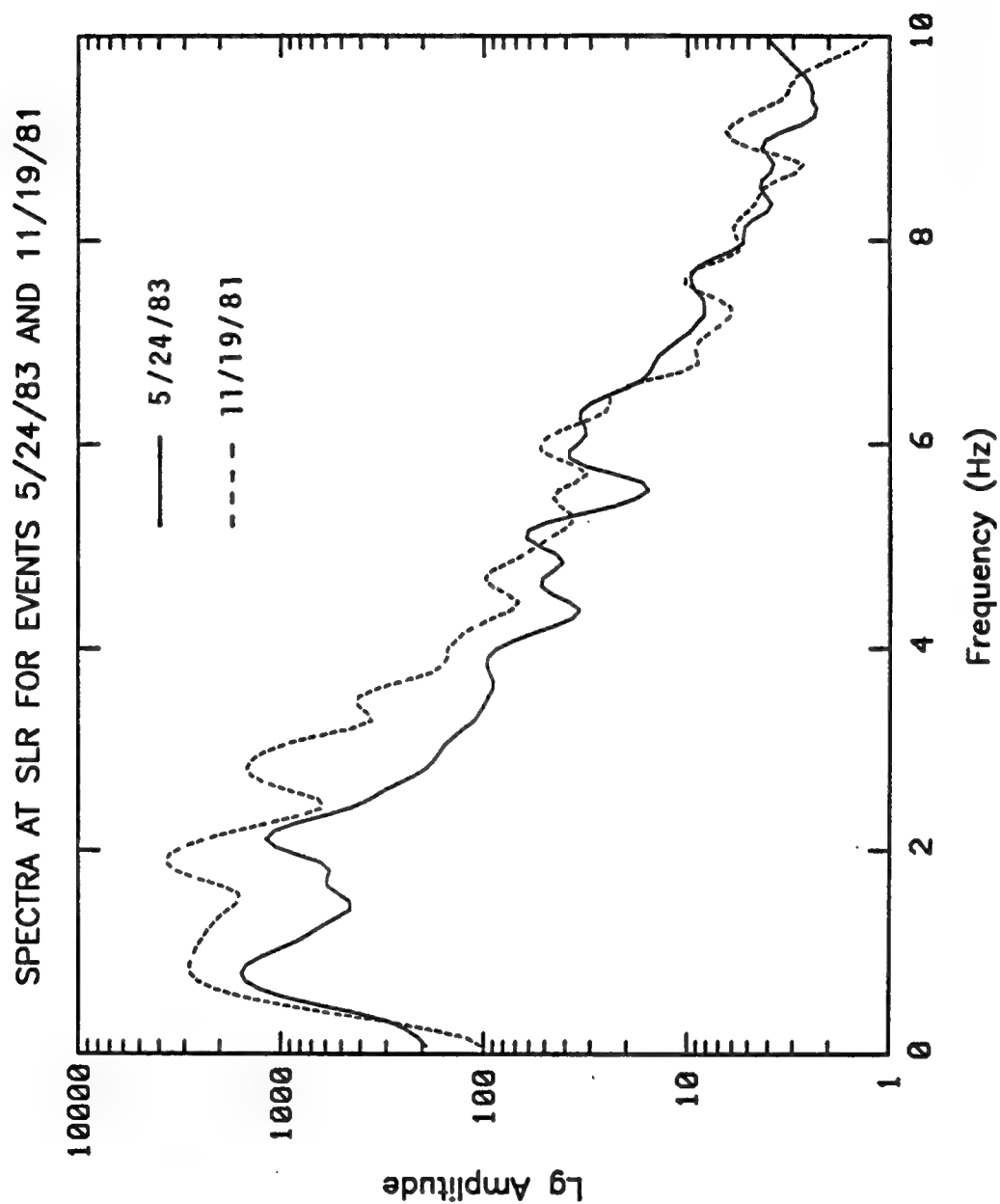
Figure 24. Comparison of Fourier spectra of the L_g signals at station SLR from two mine tremors in the Orange Free State mining area of South Africa.
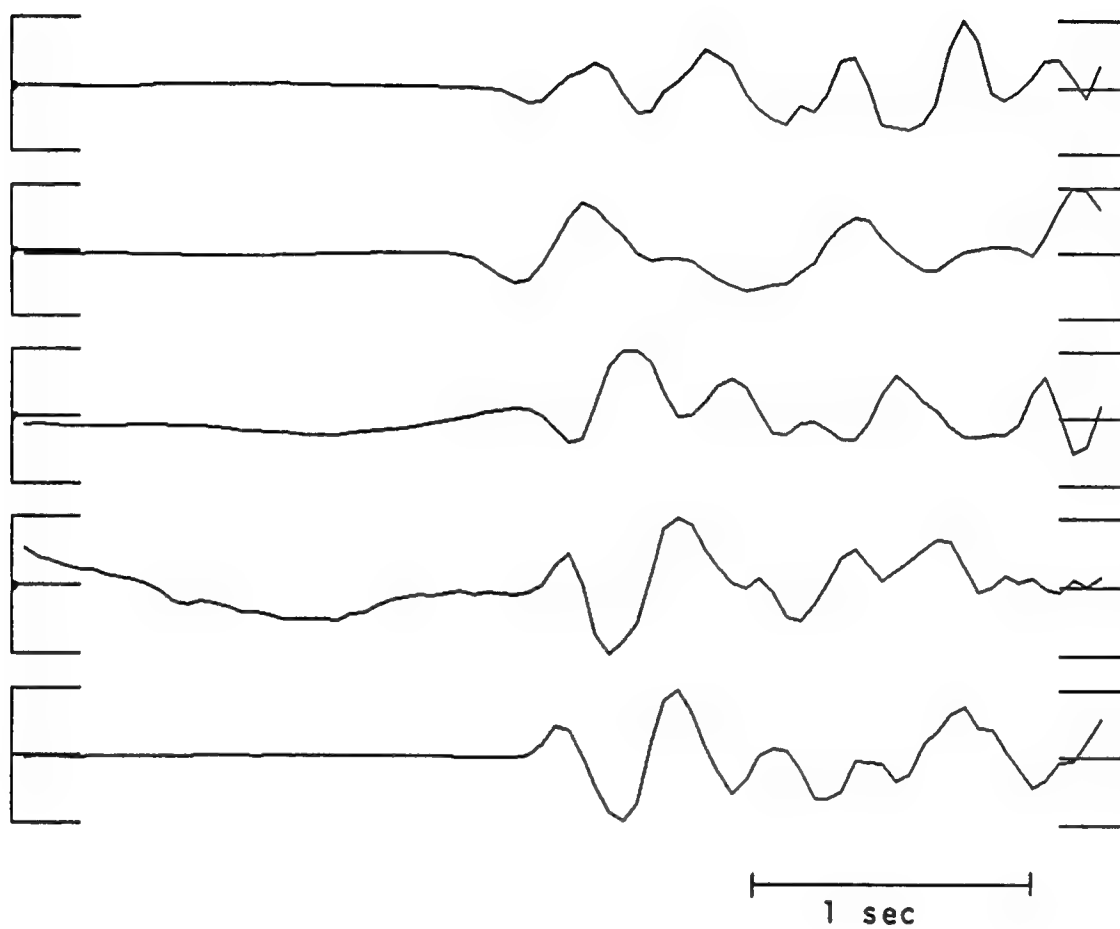
Figure 25. Initial P waveforms at station SLR for mine tremors from the Far West Rand mining district of South Africa.

rockburst events from the Far West Rand mining district (R ≈ 100 km). In two cases the first motion is clearly dilatational; in two cases it is clearly compressional; and one case is ambiguous. Mine tremor events separated by less than about 5 km show opposite first motions. It seems most likely that this observation can be best explained by a change in source mechanism between the events. It is not unreasonable to expect that such a source mechanism difference could affect the spectral behavior of the transmitted seismic signals in addition to the first motions.

A reasonable interpretation of the regional observations at SLR from events in the South African rockburst zone is that there is some degree of variability in source mechanism between events from a rather limited source area. The mechanism differences are the most likely cause of the observed P-wave first motion differences and may explain some of the spectral differences observed in regional and teleseismic signals.

5. Rockburst Mechanisms and Other Discriminant Measures

5.1 Investigation of the M_S versus m_b Discriminant

A teleseismic discriminant which has proven to be extremely valuable for distinguishing underground nuclear explosions from earthquakes involves comparison of the relative excitation of long-period ($T \approx 20$ seconds) surface waves versus short-period ($T \approx 1$ second) teleseismic body waves for different events. The discriminant measure is usually formulated in terms of a comparison of surface-wave magnitude, M_S, versus body-wave magnitude, m_b, and has been established as one of the most robust identification techniques available for shallow events (cf. OTA, 1992). Although this discriminant has been most often utilized over the years for large teleseisms, investigators (cf. Marshall and Basham, 1972; Taylor et al., 1986) have also suggested its extension to smaller events at regional distances. However, the value of the M_S-versus-m_b discriminant for application to small events, including chemical blasts and rockbursts, remains generally unestablished for the variety of potential source environments of interest under a CTBT. In particular, calibration studies in various source areas and tectonic regions would be useful in determining discriminant characteristics and validity.

In the current investigation we have applied the M_S/m_b discriminant to rather limited event samples from Central Europe and South Africa. The samples include rockbursts and earthquakes but are limited by the fact that M_S values are seldom reported for smaller events. Since the majority of earthquakes and rockbursts in these two source regions are small, M_S

estimates are not often available. This appears to be a special problem for rockbursts as events with m_b or M_L greater than 4.5 often do not have associated M_S estimates.

Figure 26 shows a sample of 12 events gleaned from the NEIC catalogs for Central Europe and South Africa for which M_S measurements were reported. The sample includes three earthquakes, and the remainder are rockbursts. In the figure we have plotted the NEIC reported M_S versus NEIC m_b for each event. For reference, we show lines for which $M_S = m_b$ and for which $M_S = m_b - 1.0$. The measurements show more than an order of magnitude of scatter. With regard to discrimination, the traditional thinking is that the more that event M_S values fall below m_b values the more likely the event is to be an explosion. For four out of the 12 events shown in Figure 26, the M_S values are within 0.3 magnitude units of m_b; they include two of the earthquakes. However, the remaining eight events have M_S values more than one-half magnitude unit lower than m_b and include four events with M_S values more than one magnitude unit lower than m_b.

Figure 27 shows a similar plot of magnitude measurements derived by averaging AEDS station magnitudes for a sample of ten events. It should be noted that some of the same events as in the preceding figure are included here and that no station corrections were applied in computing the event averages. In this case the Central European earthquake (4/13/92) falls near the $M_S = m_b$ line, but all of the rockbursts appear to be more explosion-like. Comparing just the Central European rockburst (3/13/89) and the Central European earthquake, the earthquake appears quite normal ($M_S \approx m_b$); but the rockburst looks very explosion-like ($M_S < m_b - 1.0$). Considering that both of the latter

63
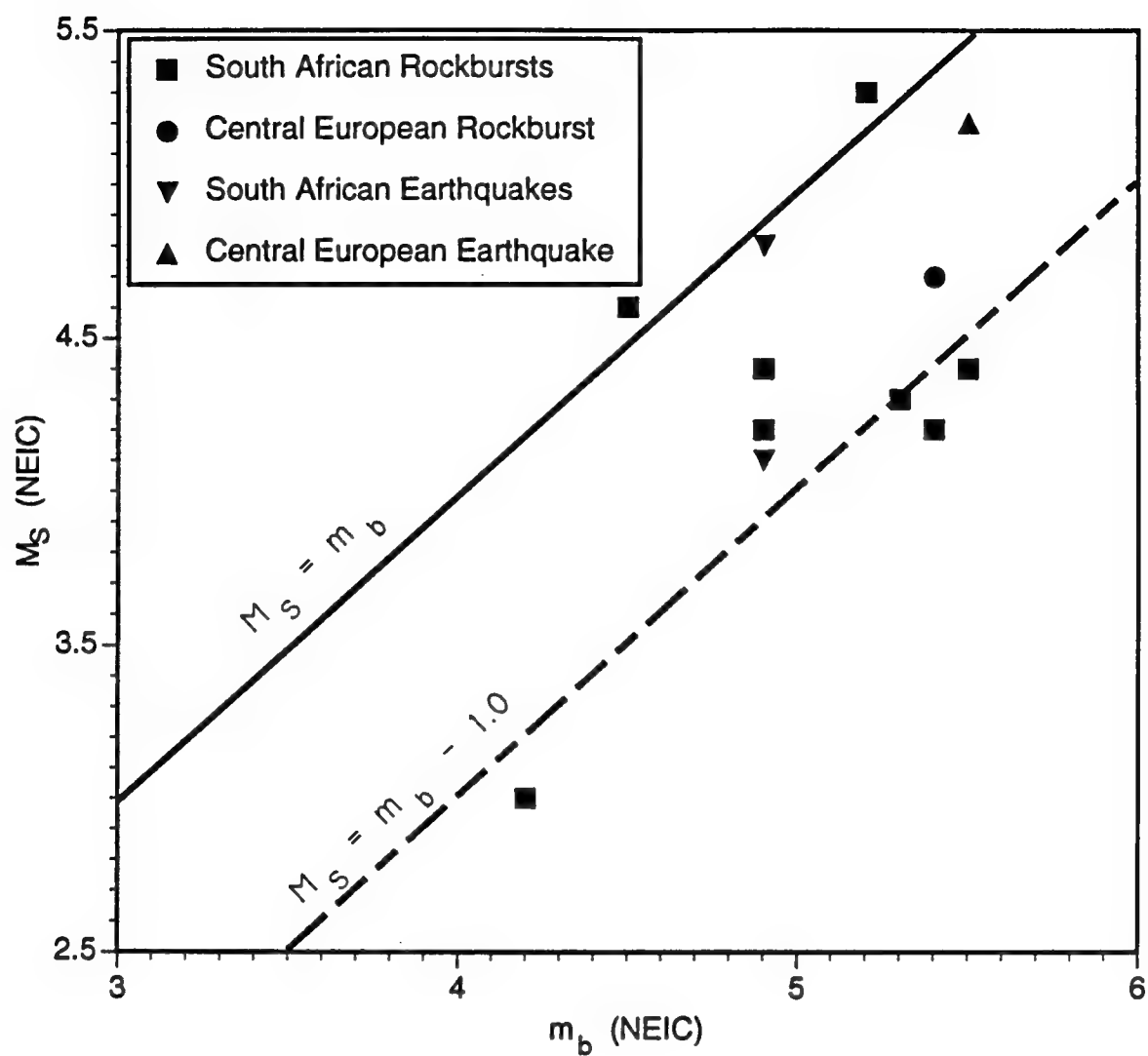
Figure 26. M_S versus m_b measurements reported in NEIC catalog for selected rockbursts and earthquakes from Central Europe and South Africa.
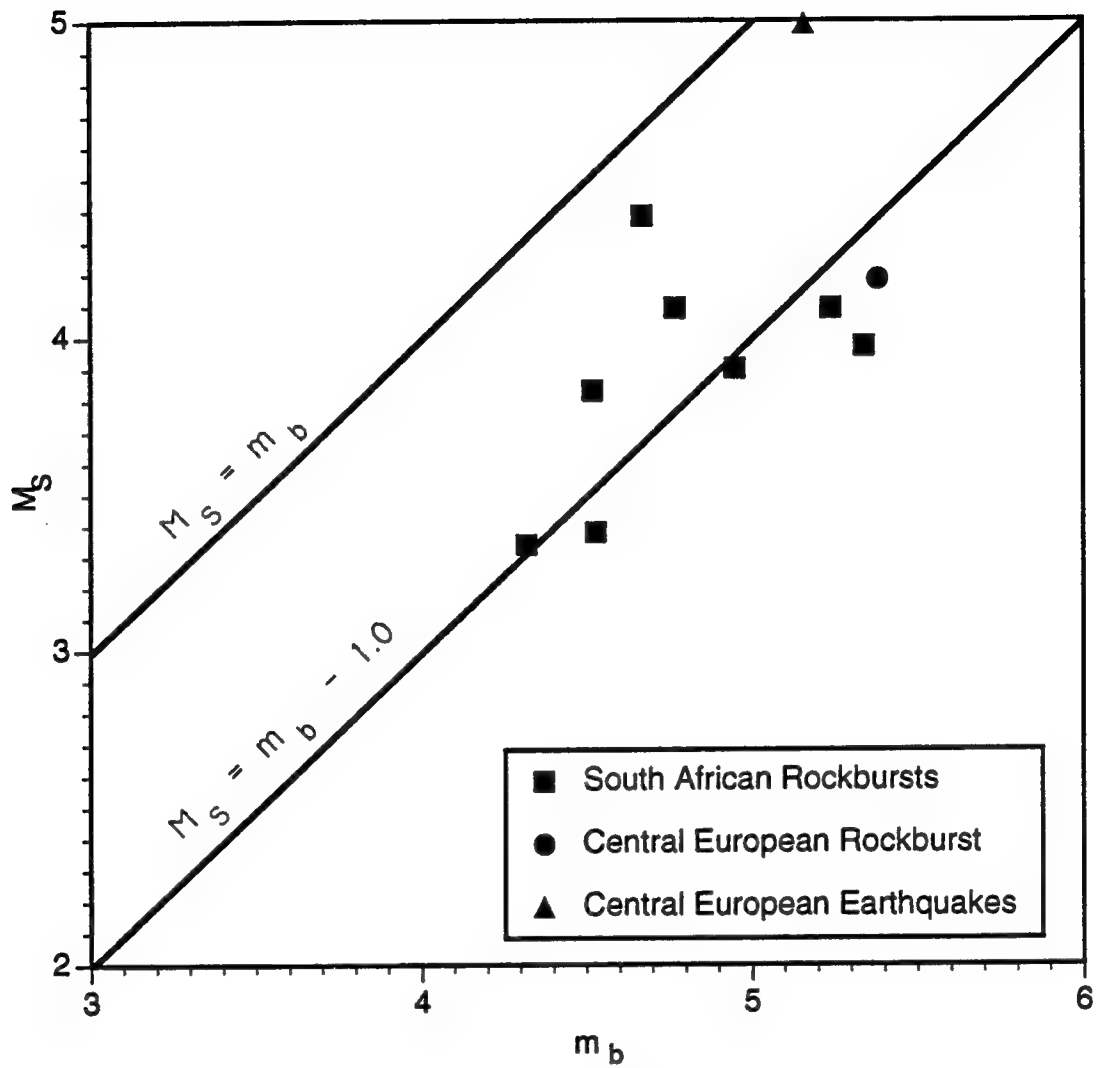
Figure 27. M_S versus m_b determined from AEDS station measurements for selected rockbursts and an earthquake from Central Europe and South Africa.

events come from essentially the same source region, it seems unlikely that path corrections would do much to compensate this difference. The observation suggests that rockbursts may tend to look more explosion-like than earthquakes with respect to the M_S/m_b discriminant. However, this conclusion is rather weak because of the limited data sample from which it is drawn, and it should probably be tested for a larger sample.

For the South African events, we did try to assemble a somewhat larger sample of M_S measurements using data recorded at station BCAO ($\Delta \approx 32°$). In our previous report (Bennett et al., 1993) we showed evidence of fairly strong long-period Rayleigh waves at BCAO from several events in our South Africa rockburst database. For a sample including 18 rockburst events with $4.2 \leq m_b \leq 5.2$, we computed surface-wave magnitudes from the long-period Rayleigh waves recorded at BCAO. The waveform segments were first filtered in a passband from 0.04 Hz to 0.06 Hz to isolate signals with periods in the vicinity of 20 seconds. Peak-to-trough vertical-component ground motion amplitudes determined from the maximum amplitude in the Rayleigh wave group velocity window were then used in the Prague formula (Bath, 1979) to calculate M_S:

$$M_S = \log (A/T) + 1.66 \log \Delta \qquad (4)$$

where A is the measured amplitude in nanometers, T is period in seconds, and Δ is epicentral distance in degrees. The results were plotted in Figure 28 versus the NEIC reported body-wave magnitude, m_b. For two events the Rayleigh waves appeared to have some interference from other events; these are marked with downward arrows suggesting the corresponding M_S estimate may be an upper bound. Although the M_S-versus-m_b measurements in Figure 28 show considerable scatter, they appear to be consistently explosion-like with

66
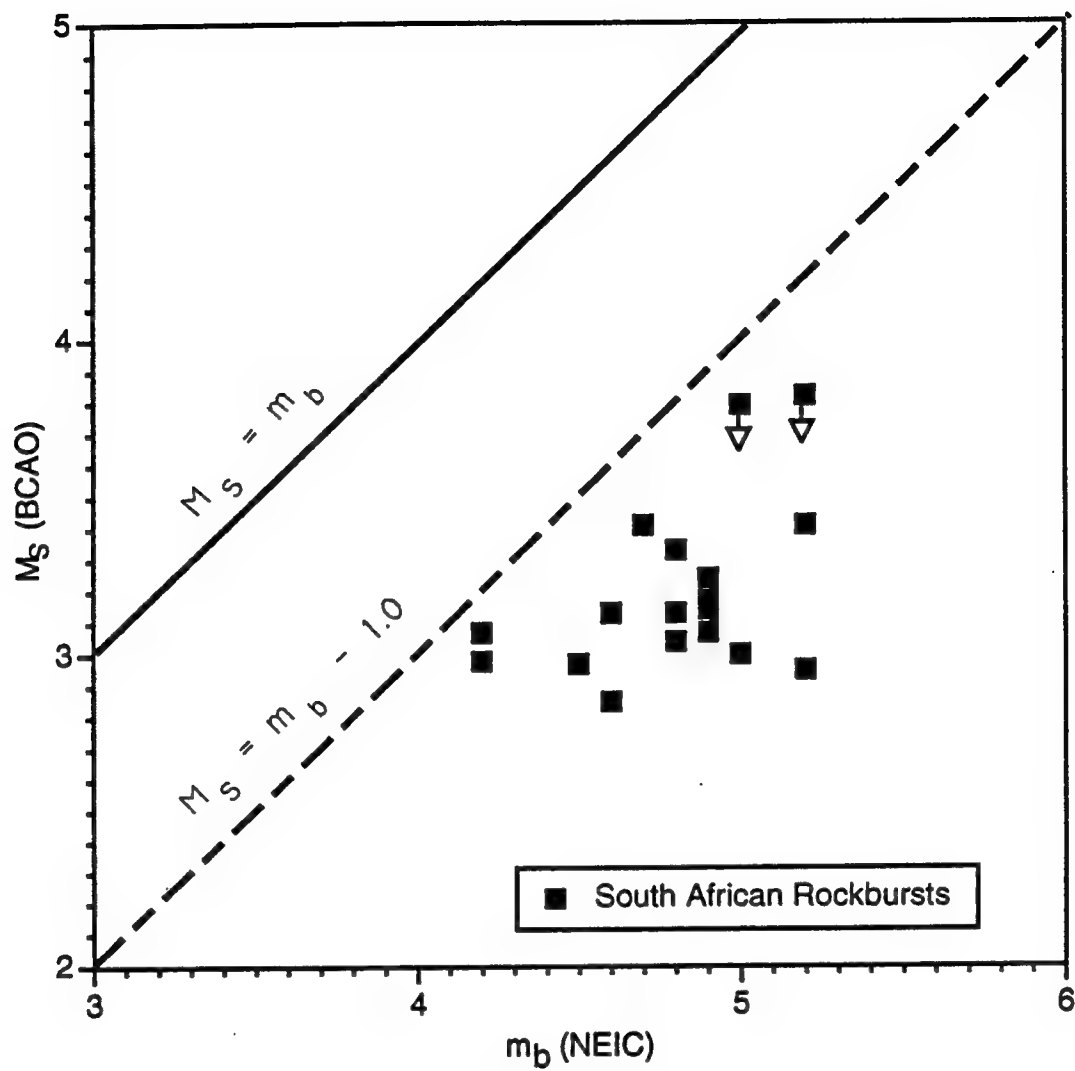
Figure 28. M_S determined from long-period Rayleigh wave measurements at station BCAO versus m_b reported by NEIC for selected South African rockbursts.

M_S values in all cases more than one magnitude unit below m_b and, in some cases, as much as two magnitude units below m_b. It should be noted here, however, that measurements are at a single station, and no station corrections have been applied. If the transmission path into BCAO is poor or the station lies on a node of the Rayleigh-wave radiation pattern, low M_S values might be expected. Additional investigations using other stations for some of the larger events and predictions based on knowledge of the focal mechanisms could help to resolve the cause for the low M_S measured for these South African rockbursts.

5.2 Rockburst Mechanisms

In our previous report (Bennett et al., 1993) we described some of the mechanisms associated with rockburst activity. Six distinct models for mining-induced seismic events were defined by Hasegawa et al. (1989). These models are (1) cavity collapse, (2) pillar burst, (3) tensile failure in the cap rock, (4) normal faulting above the stope face, (5) thrusting above or below the excavation, and (6) shallow, horizontal thrusting along layering planes above the mine roof. These various models would be expected to differ with respect to energy release and the mechanisms of seismic wave generation. Individual rockfalls or pillar-bursts would be expected to normally release only small amounts of seismic energy and to have simple vertical-force or dipole mechanisms unlike the double-couple mechanisms experienced in some other rockbursts and typical earthquakes. Although several of these models may act in combination to produce quite complex seismic mechanisms, for many rockbursts in many different source regions the mechanisms appear to be

68

dominated by shear failure similar to that in earthquakes. Furthermore, in many mining areas the ambient tectonic stress appears to contribute to the mechanism, enhancing the source energy release and controlling the rockburst process. As a result, many rockbursts throughout the world would be expected to behave in most aspects similar to shallow earthquakes with regards to seismic discrimination characteristics. However, unusual events with more complex mechanisms sometimes do occur and may be found in essentially the same source region where the simpler mechanism dominates. Some of these complex events have been large, as will be described below; and there is sometimes a close tie to mining practice.

The mechanisms of rockbursts in South Africa have been studied and analyzed more than those in any other area. The attention they have received can be attributed to several factors including the size and frequency of the mine tremors and the severe consequences of some events. In addition, the substantial seismic monitoring effort in the vicinity of South African mines provides excellent capability to resolve mechanisms and analyze the influences of mining practice. One result of this is that there is some tendency for experience gained from South African mine tremors to dominate understanding of the rockburst problem in other parts of the world. In recent years more detailed analyses have been made of rockburst mechanisms from mining areas in other geographical regions (e.g. Central Europe and Canada) which also have extensive records of such activity. In many cases these latter studies confirm the South African experience, but distinctive features also have been found in some cases.

In South Africa observations from large mine-induced events support the conclusion that such events are primarily associated with shear failure on faults or zones of weakness in the vicinity of the excavation (cf. McGarr, 1971; Spottiswoode and McGarr, 1975; McGarr et al., 1979). These large events are usually closely associated with the prevalent tectonic stress conditions in the region surrounding the mine, so that the seismic mechanisms represent the response of fractures or weaknesses adjacent to the excavation which are favorably oriented in the ambient stress field. Gay et al. (1984) argue that mining-induced energy cannot possibly account for a significant part of the total energy released during a large event. They conclude that the large mine tremors in South Africa draw from residual strain energy related to the regional tectonics.

Many small events, with magnitudes in the range $1 \leq M_L \leq 3$ also produce a quadrantal distribution of first motions, as measured on near-source arrays, which suggest that the events are the result of shear failure (cf. Spottiswoode, 1984; Potgieter and Roering, 1984). However, there have been some exceptions to this behavior even in South Africa. Rorke and Roering (1984) found that mine-tremor events with magnitudes in the range $-1.0 \leq M_L \leq 2.8$ at the Doornfontein Gold Mine did not produce quadrantal first-motion patterns but had only two lobes. In most events occurring close to the mine stope face, a rarefactional lobe occurred on the stope side of the event and a compressional lobe on the unmined side. Exceptions to the double-couple mechanism for rockbursts have also been found in Central Europe (cf. Sileny, 1989; Gibowicz et al., 1990) and in the western U.S. (cf. Wong et al., 1989; Taylor, 1992). In fact, the large German rockburst which will be described more

completely later in this section also may be an exception to the simple shear mechanism.

In our previous report (Bennett et al., 1993) we described the more typical rockburst model as a seismic event triggered when the stresses are redistributed on a tightly confined fault usually in the vicinity of the excavation. This stress redistribution, which is caused by the mining activity, induces a frictional instability on the fault causing a shear failure to spread on the fault plane and radiating seismic waves. Such a mechanism is equivalent to a double couple and produces the typical quadrantal radiation pattern. The displacement spectrum from this type of source consists of a flat low-frequency trend, a descending intermediate trend with slope proportional to ω^{-2} to ω^{-3} and an upper frequency limit controlled by either attenuation or source properties (cf. Madariaga, 1979). Studies of the spectral behavior of South African mine tremors by McGarr et al. (1990) and Battis (1992) suggest that this double-couple rupture model satisfactorily explains the events which they analyzed. However, in some cases there were indications in their results that the rupture process was more complex probably because of multiple rupture events.

In a more general approach to the problem of mining-induced seismic events, Kuhnt et al. (1989) distinguished two different types of rockbursts: (1) a tectonic type related to induced fault movement in the ambient tectonic stress field (similar to the typical South African mechanism just described), and (2) a static type which is more closely connected to mining activity and not dependent on tectonic stress. For this latter model Kuhnt et al. formulated representations of the process in terms of both barrier and asperity models. In the barrier model the surroundings of the pillars act as barriers to propagation of a crack outward

71

from the stope area. In the asperity model the pillars form asperities which concentrate stresses and which ultimately fail under the induced stress to produce the tremor. In either model, multiple pillars may be affected in a single rockburst and, depending on their locations and properties, the resulting rockburst process may be quite complex. The studies indicate that the mining practice can to some degree control the process and lead to variations in the source between events. It has not been determined to what extent the complexity in the model may contribute to the observed seismic signals. Some of the studies already cited suggest that these kinds of complexity are most likely to affect small events. However, there may be some mining situations where large events may have added complexity.

5.3 Mechanism of the 1989 Völkershausen, Germany Rockburst

In several preceding sections of this report, we showed observations from a large rockburst in Central Europe. This event occurred on March 13, 1989 near Völkershausen, Germany and had a magnitude of 5.4 m_b and focal depth near 1 km. The rockburst occurred at the Ernst Thaelmann Potash Mine and produced considerable damage to buildings in the area and some loss of life to miners. this event was widely recorded on local and regional seismic networks as well as at far-regional and teleseismic stations. A few reports have been published regarding the mining conditions and seismic measurements associated with this event (e.g. Ahorner, 1989; Bormann, 1992; Bowers and Pearce, 1992; Minkley, 1993). We review here the source models and some apparently conflicting information observed from the observed seismic signals.

Unlike the typical South African mine tremor, the Völkershausen rockburst is thought to have been produced by the nearly simultaneous collapse of multiple mine pillars (cf. Ahorner, 1989; Minkley, 1993). This event was apparently triggered when an attempt was made to mine-out some remnant pillars in the mine without giving appropriate engineering attention to effects on the surrounding stress field. However, the consequence was far greater than failure of a few of the surrounding pillars. In this case it has been reported that about 3200 pillars collapsed within a very short time span (cf. Bormann, 1992). Figure 29 shows a schematic model of the Völkershausen rockburst along with an approximate energy calculation to estimate the energy released in the event. The pillar collapse occurred at depths of about 850 - 900 m. Minkley (1993) shows results obtained from displacement meters at the surface above the mine which indicate that a large area subsided. The subsidence area appears to extend over the surface for 2 - 3 km laterally. The displacement meter results further indicate that maximum subsidences at the earth's surface were from 0.8 - 1.0 m and that the process was generally completed within a few seconds.

In Figure 29 we performed a simplified calculation to determine the potential energy loss due to subsidence by 0.7 m of a block approximately 3 km by 3 km. We also calculated the seismic energy from the Gutenberg-Richter relationship associated with a seismic event having a body-wave magnitude of 5.4 m_b. The calculation suggests that the potential energy available from the mine collapse process, in this case, is quite large. A seismic efficiency of only about 0.5 percent would be needed to produce the observed body-wave magnitude for this event. Even if the average subsidence was assumed to be only half as great or the lateral extent was reduced by 50 percent, reasonable

Not To Scale

Room and Pillar Mining in Seam

$\sim$3 km

0.7 m

900 m
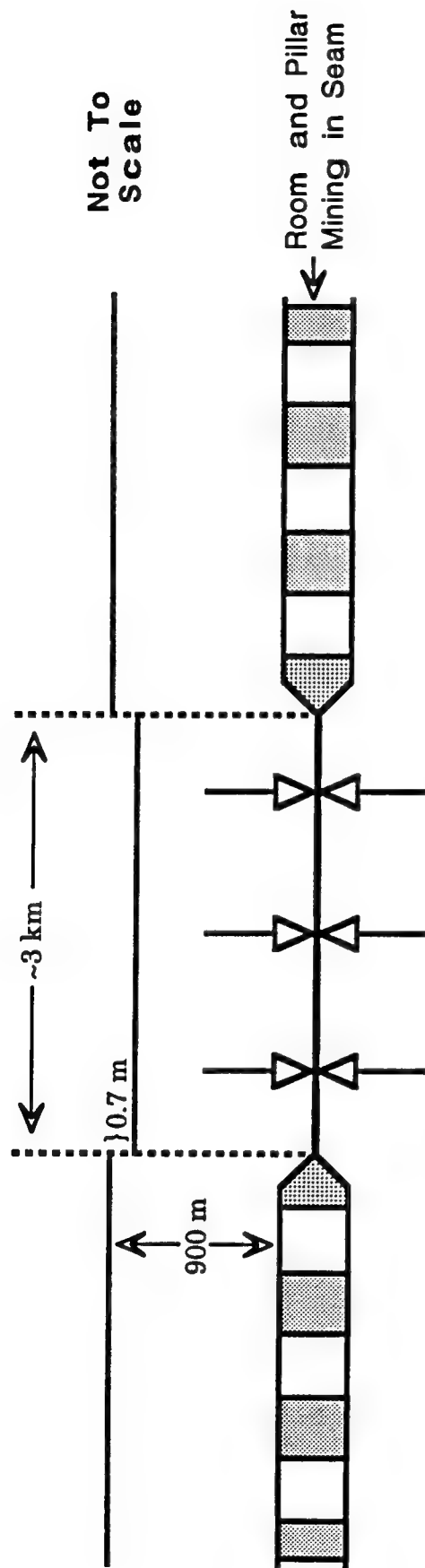
Potential Energy $E_p \approx 1.1 \times 10^{21}$ ergs

Seismic Energy $E_s = 10^{5.8 + 2.4 \, m_b}$ (Gutenberg - Richter)

$$= 10^{18.76} \approx 5.7 \times 10^{18} \text{ ergs}$$

Seismic Efficiency $e_s = \dfrac{E_s}{E_p} \approx \dfrac{5.7 \times 10^{18}}{1.1 \times 10^{21}} = 0.52\%$

Figure 29. Schematic of the 1989 Völkershausen, Germany rockburst (5.4 m_b) mechanism and the associated energy relations.

74

seismic efficiencies in the 1 - 2 percent range could still be obtained. This calculation indicates that, in this case, the mine collapse was probably large enough to produce the observed magnitude of 5.4 m_b without having to draw on tectonic strain energy. Similar calculations of this type could be performed easily to estimate the extent of mine collapse required to produce events of various magnitudes. More sophisticated model studies would also be useful for analyzing details of this and other rockburst processes and to estimate the expected ground motions at local and regional distances from such events.

With regard to seismic signal generation, Ahorner (1989) has suggested that the Völkershausen rockburst source could be represented as an implosion. For the collapse of individual pillars, the vertical motion vectors above and below are directed inward toward the pillar. Horizontal motions are directed outward from the pillar, but these motions are into the open rooms between pillars and do not transmit as seismic waves. The model is not strictly an implosion (for which horizontal motions would also be directed inward), but rather an inward vertical dipole. The P–wave first motions produced by this source model would be expected to correspond to dilatations at all stations. To test the model Ahorner studied the P-wave signals at a regional network of about 50 seismic stations out to ranges of 380 km. The sense of the first motions observed at these stations are shown on the left of Figure 30, as plotted by Ahorner. All the first motions, corresponding to P_g and P_n phases, are dilatational at all azimuths which apparently agrees with the proposed "implosional" source model.

As a further test of the seismic mechanism of this event, we analyzed the first motions for all stations reported in the ISC Bulletin. These observations

Figure 30. Comparison of P-wave first motions for the March 13, 1989 Völkershausen rockburst reported by Ahorner (1989) from observations at a near-regional/regional station network (left) and as reported in the ISC Bulletin from all stations (right). Numerous compressional first motions at ISC stations may be indicative of signal-to-noise limitations which prevent detection of the initial pillar failure.

include 114 stations at ranges from $\Delta < 1^o$ to $\Delta > 83^o$ and incorporate some, but not all, of the stations used by Ahorner. These first motions are plotted on the right of Figure 30. As can be seen in the plot, both compressional and dilatational first motions have been reported from these stations. Of the reported first motions 62 are dilatational and 52 are compressional. Only 7 of the 35 P_n phases (reported for $\Delta < 8^o$) are compressional, and only 7 of the 30 P phases reported for $\Delta > 30^o$ are dilatational. There appears to be no clear mechanism pattern in the distribution of the first motions. One explanation for the discrepancy between the left and right plots in Figure 30 could be inaccurate first motion reports, presumably from the ISC Bulletin. Such problems arise due to inconsistent identifications of the first motions in low S/N conditions. However, we cannot asses the validity of this argument without additional knowledge of the actual waveforms which is beyond the scope of the current investigation. A related explanation of the distribution of first motions in the right-hand plot might be that the Völkershausen rockburst was a complex event. Near-in stations and those with high S/N conditions would have reported the initial "implosional" phase of the collapse. However, at some slightly later time, the more distant teleseismic stations and those with lower S/N conditions might have seen a second, possibly larger, event. This second event could have been associated with an outward vertical dipole phase caused by closure between the roof and floor of the mine or by some tectonic stress release. The latter might also explain the normal, dip-slip double-couple source reported by Bowers and Pearce (1992) for this event based on relative amplitude analyses of initial and secondary phases at two teleseismic station arrays. The additional theoretical studies of the mechanism of this rockburst, as noted above, along

77

with detailed analyses of the observed regional and teleseismic signals would be useful in resolving the processes contributing to the Völkershausen rockburst.

5.4 Implications for Identification and Control

In our previous report (Bennett et al., 1993) we noted that many rockbursts have mechanisms similar to earthquakes and that, in general, discrimination procedures which are effective for earthquakes should also work for rockbursts. It was further suggested that, since many rockbursts are small, regional discrimination techniques may be key to their identification. We considered there a variety of traditional discriminants including focal depth, M_S versus m_b, sense of first motion, spectral scalloping, and S or L_g versus P excitation. Additional comments on the conclusions presented there are appropriate in the light of the findings of this current report.

First, with regard to focal depth, rockbursts and underground nuclear explosions occur at about the same focal depths while earthquakes are often located much deeper. Depth estimation techniques, such as depth phases, P-wave location, and the Wadati technique using S - P times, would not be expected to be able to reliably determine any significant differences in focal depths between rockbursts and underground nuclear explosion tests. So, in this respect rockbursts behave differently from earthquakes and may complicate utilization of some standard nuclear explosion discrimination techniques which rely on focal depth estimation.

Second, with regard to the M_S versus mb discriminant, we noted above that M_S is not often determined for rockburst events. Many of the events are

small and not very well recorded on long-period instruments. This might be due to a reduced excitation of long-period (20-second) Rayleigh waves for the small events. For even the largest rockburst events, we found that the long-period Rayleigh waves were relatively weak. Thus, M_S measurements reported for Central European and South African rockbursts were frequently on the order of one-magnitude unit lower than m_b. Furthermore, the M_S values which we estimated at BCAO for our selected sample of South African rockbursts were from one to two magnitude units less than m_b. The rockbursts then appear to be explosion-like with respect to the M_S versus m_b discriminant although the degree of the M_S - m_b difference might be exaggerated by the small number of stations and lack of station corrections in our magnitude estimates. In any case, application of the M_S/m_b discriminant to small events including rockbursts would appear to require some assessment of these excitation differences and enhancement of M_S measurement capability probably using a network of regional stations.

Two other discrimination methods, first motion and complexity, appear to offer some promise for distinguishing rockbursts from other source types. P-wave first motions from rockbursts would be expected to differ from the uniform compressions expected from explosions. Shear rockbursts should produce quadrantal radiation patterns similar to earthquakes; however, other rockburst sources may be less regular. In particular, we saw examples of rockbursts with very complex first motion patterns which would not fit an earthquake rupture model. Furthermore, P waves from rockbursts frequently appear to be emergent and complex, which makes first motion sometimes hard to determine. The complexity of the rockburst signal does, however, lend itself to an alternate

discriminant measure. More complex signals in earthquakes and rockbursts should provide some distinction from relatively simple nuclear explosion sources. In fact, we found evidence in this study of complexity in rockburst signals even greater than in earthquakes. However, additional testing of proposed parametric measures of complexity are needed to verify this discriminant for rockbursts as well as earthquakes.

With regard to regional signals, we found that S/P spectral ratios fro rockbursts tended to be lower than those of earthquakes but not as low as those of blasts. In addition, there was evidence of differences in the L_g/P ratio behavior as a function of frequency for the different source types. Earthquake and rockburst ratios tended to increase with frequency while blast ratios decreased. We also found that regional P for the blasts appeared to be enhanced at high frequencies compared to other source types. Additional studies are needed to confirm this behavior in different source areas and for larger event samples; however, these initial results offer promise that regional spectra may provide a valuable discriminant measure for different source types.

Finally, a particularly interesting aspect of rockbursts bearing on the nuclear explosion test evasion problem is that rockburst sources appear to be controllable. The idea of using a natural earthquake to conceal a clandestine nuclear explosion test was originally dismissed because the potential evader has no control over the timing, location, and size of the earthquake and, therefore, cannot plan for his test. However, there is accumulating evidence in the mining engineering literature that rockburst sources can be predicted to some degree and controlled. In our previous report (Bennett et al., 1993) we noted that mining engineers have developed finite element techniques which

enable accurate stress analysis and prediction in the rock surrounding mining excavations. These and corroborative monitoring programs provide the capability to predict rockburst occurrence and level with some accuracy within specific mining areas. Case histories have been reported where addition or removal of supports were used to reduce stress level below some critical threshold or to increase it to the point of inducing a rockburst in some selected magnitude range.

Therefore, a viable evasion scenario appears to be that a small or decoupled nuclear explosion test might be concealed in a triggered rockburst event. Given the widespread nature of rockburst occurrence in mines, such a scenario might be carried out in any number of countries. Assuming that even large rockbursts might be predictable and controllable, the companion nuclear explosion could be not only difficult to identify but its seismic signals might not even be detected. Theoretical model studies could be useful in evaluating this scenario and identifying possible monitoring strategies for specific source areas.

6. Summary and Conclusions

6.1 Research Summary

As a result of changing emphases in the field of nuclear explosion monitoring in recent years, alternate types of seismic sources have taken on new significance. The research described here has focussed on rockbursts, or mining-induced tremors, because they represent a significant class of events which has received little prior attention with regards to seismic discrimination. Rockbursts are important to the seismic discrimination problem because they are frequent, occur in aseismic as well as seismic areas, may be large, and can be controlled. This research program was designed to investigate characteristics of rockbursts which might help facilitate their identification in the context of nuclear explosion test monitoring.

Although rockbursts occur in many areas throughout the world, for this study we focussed on two particular regions: Central Europe and South Africa. In both of these source regions, there have been frequent reports of rockbursts and several of these have been large. As a result, good waveform data from high quality stations can be obtained for several events from these areas. For both Central Europe and South Africa, we attempted to assemble a database of representative events, including rockbursts as well as contrasting source types, which could be used in discrimination analyses. Digital seismic waveforms were collected for 60 events from Central Europe and 79 events from South Africa. The waveforms included high-quality data from SRO, ASRO, DWWSSN, ARPA regional arrays, Soviet IRIS, GSETT-2, and AEDS stations. The events covered a magnitude range from 2.0 to 5.5 m_b. In all cases seismic records

with good signal-to-noise conditions were found for at least one station. The data for larger events included many teleseismic waveforms from a global network of stations, while the smaller events provided useful data at only a few far-regional or regional stations.

For these data a variety of time-domain and spectral analyses were performed on the waveforms for selected events. For teleseismic signals we focussed on the P-wave segments and the long-period Rayleigh waves at selected stations. We reviewed the complexity of the P waves and compared P-wave spectral measurements between events. We also analyzed the M_S-versus-m_b discriminant for larger events for which data were available. For the far-regional and regional waveforms, we investigated the relative excitation of P, S, and L_g signals in both the time and spectral domains for selected events. We also looked at sense of first motions as a possible discriminant for the rockbursts. In these studies we attempted to select events and stations which would reduce to some degree propagation path effects and, therefore, provide indications of source differences. Comparisons were made between different source types to identify potential distinguishing characteristics of the signals and between similar source types to identify variability in the source or possible path influences.

In addition to the data analyses, we investigated the mechanisms and control of rockburst events. In these investigations we reviewed the technical literature to identify common and contrasting features in the source mechanisms of rockbursts. We then sought to identify what implications different mechanisms and source characteristics would have on some typical discriminant measures. As part of this review of rockburst mechanisms, we also

considered predictability and control of rockburst events by mining practice and the implications of such capability for clandestine nuclear explosion testing.

6.2 Principal Conclusions

One important finding of this research program is that rockbursts occur in hardrock mining areas throughout the world. In many areas the events are frequent, and they may be large. The widespread nature of this kind of activity indicates that they could pose a significant problem for CTBT or proliferation monitoring. In fact, in many parts of the world mining-induced events may present more of a problem to discrimination monitoring than commercial blasting operations.

Among the techniques for distinguishing rockbursts from other source types, the spectral differences in seismic signals appear to be most promising. The Lg/Pg spectral ratios observed at regional station GRFO for different Central European source types at similar regional distances suggest that the ratio tends to be largest for earthquakes, somewhat smaller for rockbursts, and much smaller for blasts; however, there was some evidence of frequency dependence. The individual phase spectra show a tendency for the blast P to be richest in high frequencies and for the earthquake P to be enriched at high frequencies relative to the rockburst. The available far-regional and teleseismic signals from larger Central European and South African events showed a similar tendency for P to be enriched at high-frequencies for earthquakes relative to rockbursts. This trend was strongest for the largest Central European events. Evidence of differences in spectral behavior for some far-regional events and effects of differences in propagation path at regional and far-

regional stations will require additional investigation before drawing conclusions about source variability between individual rockbursts.

With regard to other techniques for discriminating rockbursts, rockbursts are like explosions in that they occur at comparable focal depths; so depth-based discrimination techniques would not be expected to provide any distinction. However, some characteristics indicate that rockbursts should behave as earthquakes and, therefore, might be distinguished from nuclear explosion tests using the same techniques used to separate earthquakes. In particular, rockbursts which correspond to release of tectonic stress on pre-existing zones of weakness, or faults, near the excavation should behave like earthquakes. In fact, we found examples in our comparisons of regional signals for South African events that S/P ratios in the time domain intermingled for rockbursts and earthquakes.

However, some rockbursts are more complex and may include non-earthquake processes such as rock fall or pillar failure. We found examples in both the Central European and South African databases where the teleseismic, and also regional, P signals were at least as complex for rockbursts as for earthquakes from the same region. Such complexity in rockburst signals may be useful as a discriminant and should be investigated further. The complexity seen in the rockburst source along with the emergent character found in many regional P signals from rockbursts tends to mitigate against the value of sense of first motion as a discriminant. In South Africa we found examples where the sense of first motion appeared to change on regional records from rockbursts in the same source area. Consequently, some rockburst events are likely to produce anomalous first motion patterns.

One other discrimination technique which appears to be problematic for rockbursts is M_S versus m_b. In the first place, many of the events are small and would require some kind of regional measurement of the magnitudes. Furthermore, the evidence we analyzed for even large rockbursts indicated a tendency for rockbursts to generate relatively weak M_S. This explosion-like behavior for the M_S/m_b discriminant needs further study including more stations and other source areas.

Finally, with regard to the potential use of rockbursts to conceal clandestine nuclear testing, there is evidence in the mining literature that rockburst activity can be controlled by engineering techniques. Application of finite element procedures to specific mining areas enables the engineer to accurately predict stress conditions in the surrounding rock. Case histories indicate that addition or removal of supports can be used to reduce stress level below some threshold or increase it to induce a rockburst in a particular magnitude range. A viable evasion scenario appears to be that a small or decoupled nuclear explosion test might be concealed in a triggered rockburst. Additional analyses are needed to determine the maximum size of events which can be controlled in this manner. If large rockbursts can be controlled. a simultaneously detonated nearby nuclear explosion would be difficult to detect and identify.

7. References

Ahorner, L. (1989). "Seismologische Untersuchung des Gebirgsschlages am 13. Marz 1989 im Kalisalzbergbau bei Völkershausen, DDR," Gluckauf-Forshungshefte, 50, pp. 224-230.

Bath, M. (1979). Introduction to Seismology, Birkhauser Verlag, Basel.

Battis, J. C. (1992). "Source Modelling of South African Mine Tremors," (Abstract), Seismological Research Letters, 63, p. 20.

Bennett, T. J., A. K. Campanella, J. F. Scheimer, and J. R. Murphy (1992). "Demonstration of Regional Discrimination of Eurasian Seismic Events Using Observations at Soviet IRIS and CDSN Stations," S-CUBED Report No. SSS-FR-92-13150, PL-TR-92-2090, ADA253275.

Bennett, T. J., J. F. Scheimer, A. K. Campanella, and J. R. Murphy (1993). "Seismic Discrimination of Rockbursts for Use in Discrimination," S-CUBED Report No. SSS-DTR-93-13792, PL-TR-93-2059, ADA266063.

Bormann, P. (1992). "Analysis of the Strong Multiple Mining Event of 13 March 1989 at Volkershausen, Germany," (Abstract), Paper Presented at Meeting of European Geophysical Society.

Bowers, D., and R. G. Pearce (1992). "An Interpretation of the Volkershausen Event of 13th March 1989 From Teleseismic Observations," (Abstract), Paper Presented at Meeting of European Geophysical Society.

Gay, N. C., D. Spencer, J. J. van Wyk, and P. K. van Der Haver (1984). "The Control of Geological and Mining Parameters on Seismicity in the Klerksdorp Gold Mining District," in Proc. Ist Int. Congress on Rockbursts and Seismicity in Mines, SAIMM, Johannesburg, pp.107-120.

Gibowicz, S. J. (1984). "The Mechanism of Large Mining Tremors in Poland," in Proc. Ist Int. Congress on Rockbursts and Seismicity in Mines, SAIMM, Johannesburg, pp. 17-28.

Gibowicz, S. J.,H.-P. Harjes, and M. Schafer (1990). "Source Parameters of Seismic Events at Heinrich Robert Mine, Ruhr Basin, Federal Republic of Germany: Evidence for Non-Double-Couple Events," Bull. Seism. Soc. Am., 80, pp. 88-109.

Hasegawa, H. S., R. J. Wetmiller, and D. J. Gendzwill (1989). "Induced Seismicity in Mines in Canada - An Overview," Pageoph, 129, pp 423-453.

Kuhnt, W., P. Knoll, H. Grosser, and H. J. Behrens (1989). "Seismological Models for Mining-Induced Seismic Events," Pageoph, 129, pp. 513-521.

Madariaga, R. (1979). "On the Relation Between Seismic Moment and Stress Drop in the Presence of Stress and Strength Heterogeneity," J. Geophys. Res, 84, pp. 2243-2250.

Marshall, P. D., and P. W. Basham (1972). "Discrimination Between Earthquakes and Underground Explosions Employing an Improved M_S Scale," Geophys. J., 28, pp. 431-458.

McGarr, A. (1971). "Violent Deformation of Rock Near Deep-Level, Tabular Excavations - Seismic Events," Bull. Seism. Soc. Am., 61, pp. 1453-1466.

McGarr, A., S. M. Spottiswoode, and N. C. Gay (1979). "Observations Relevant to Seismic Driving Stress, Stress Drop and Efficiency," J. Geophys. Res., 84, pp. 2251-2261.

McGarr, A., J. Bicknell, J. Churcher, and S. Spottiswoode (1990). "Comparison of Ground Motion from Tremors and Explosions in Deep Gold Mines," J. Geophys. Res., 95, pp. 21,777-21,792.

Minkley, W. (1993). "Zum Herdmechanismus von Großen Seismischen Ereignissen im Kalibergbau," Preprint of Paper Submitted to Jahr.Deutschen Geophysikalischen Gesellschaft.

Office of Technology Assessment (1988). Seismic Verification of Nuclear Testing Treaties, U. S. Congress OTA Report No. OTA-ISC-361.

Potgieter, G. J., and C. Roering (1984). "The Influence of Geology on the Mechanisms of Mining-associated Seismicity in the Klerksdorp Gold-field," Proc. 1st Int. Cong. on Rockbursts and Seismicity in Mines, Johannesburg, pp. 45-50.

Rorke, A. J., and C. Roering (1984). "Source Mechanism Studies of Mine-induced Seismic Events in a Deep-level Gold Mine," Proc. 1st Int. Cong. on Rockbursts and Seismicity in Mines, Johannesburg, pp.51-55.

Sileny, J. (1989). "The Mechanism of Small Mining Tremors from Amplitude Inversion," Pageoph, 129, pp. 309-324.

Spottiswoode, S. M. (1984). "Source Mechanisms of Mine Tremors at Blyvooruitzicht Gold Mine," Proc. 1st Int. Cong. on Rockbursts and Seismicity in Mines, Johannesburg, pp.29-37.

Spottiswoode, S. M., and A. McGarr (1975). "Source Parameters of Tremors in a Deep-Level Gold Mine," Bull. Seism. Soc. Am., 65, pp. 93-112.

Taylor, S. R., M. D. Denny, E. S. Vergino, and R. E. Glaser (1989), "Regional Discrimination Between NTS Explosions and Western U.S. Earthquakes," Bull. Seism. Soc. Am., 79, pp. 1142-1176.

Taylor, S.R. (1992). "False Alarms and Mine Seismicity: An Example from the Gentry Mountain Mining Region, Utah," Los Alamos National Laboratory Report No. LAUR -92-3276.

Wong, I. G. , J. R. Humphrey, J. A. Adams, and W. J. Silva (1989). "Observations of Mine Seismicity in the Eastern Wasatch Plateau, Utah, U.S.A.: A Possible Case of Implosional Failure," Pageoph, 129, pp. 369-405.

Prof. Thomas Ahrens
Seismological Lab, 252-21
Division of Geological & Planetary Sciences
California Institute of Technology
Pasadena, CA 91125

Prof. Keiiti Aki
Center for Earth Sciences
University of Southern California
University Park
Los Angeles, CA 90089-0741

Prof. Shelton Alexander
Geosciences Department
403 Deike Building
The Pennsylvania State University
University Park, PA 16802

Prof. Charles B. Archambeau
University of Colorado
JSPC
Campus Box 583
Boulder, CO 80309

Dr. Thomas C. Bache, Jr.
Science Applications Int'l Corp.
10260 Campus Point Drive
San Diego, CA 92121 (2 copies)

Prof. Muawia Barazangi
Cornell University
Institute for the Study of the Continent
3126 SNEE Hall
Ithaca, NY 14853

Dr. Jeff Barker
Department of Geological Sciences
State University of New York
 at Binghamton
Vestal, NY 13901

Dr. Douglas R. Baumgardt
ENSCO, Inc
5400 Port Royal Road
Springfield, VA 22151-2388

Dr. Susan Beck
Department of Geosciences
Building #77
University of Arizona
Tuscon, AZ 85721

Dr. T.J. Bennett
S-CUBED
A Division of Maxwell Laboratories
11800 Sunrise Valley Drive, Suite 1212
Reston, VA 22091

Dr. Robert Blandford
 AFTAC/TT, Center for Seismic Studies
1300 North 17th Street
Suite 1450
Arlington, VA 22209-2308

Dr. Stephen Bratt
ARPA/NMRO
3701 North Fairfax Drive
Arlington, VA 22203-1714

Dale Breding
U.S. Department of Energy
Recipient, IS-20, GA-033
Office of Arms Control
Washington, DC 20585

Dr. Lawrence Burdick
C/O Barbara Wold
Dept of Biology
CA Inst. of Technology
Pasadena, CA 91125

Dr. Robert Burridge
Schlumberger-Doll Research Center
Old Quarry Road
Ridgefield, CT 06877

Dr. Jerry Carter
Center for Seismic Studies
1300 North 17th Street
Suite 1450
Arlington, VA 22209-2308

Dr. Martin Chapman
Department of Geological Sciences
Virginia Polytechnical Institute
21044 Derring Hall
Blacksburg, VA 24061

Mr Robert Cockerham
Arms Control & Disarmament Agency
320 21st Street North West
Room 5741
Washington, DC 20451,

Prof. Vernon F. Cormier
Department of Geology & Geophysics
U-45, Room 207
University of Connecticut
Storrs, CT 06268

Prof. Steven Day
Department of Geological Sciences
San Diego State University
San Diego, CA 92182

1

Dr. Zoltan Der
ENSCO, Inc.
5400 Port Royal Road
Springfield, VA 22151-2388

Dr. Stanley K. Dickinson
AFOSR/NM
110 Duncan Avenue
Suite B115
Bolling AFB, DC 20332-6448

Prof. Adam Dziewonski
Hoffman Laboratory, Harvard University
Dept. of Earth Atmos. & Planetary Sciences
20 Oxford Street
Cambridge, MA 02138

Prof. John Ebel
Department of Geology & Geophysics
Boston College
Chestnut Hill, MA 02167

Dr. Petr Firbas
Institute of Physics of the Earth
Masaryk University Brno
Jecna 29a
612 46 Brno, Czech Republic

Dr. Mark D. Fisk
Mission Research Corporation
735 State Street
P.O. Drawer 719
Santa Barbara, CA 93102

Prof. Donald Forsyth
Department of Geological Sciences
Brown University
Providence, RI 02912

Dr. Cliff Frolich
Institute of Geophysics
8701 North Mopac
Austin, TX 78759

Dr. Holly Given
IGPP, A-025
Scripps Institute of Oceanography
University of California, San Diego
La Jolla, CA 92093

Dr. Jeffrey W. Given
SAIC
10260 Campus Point Drive
San Diego, CA 92121

Dr. Dale Glover
Defense Intelligence Agency
ATTN: ODT-1B
Washington, DC 20301

Dr. Indra N. Gupta
Multimax, Inc.
1441 McCormick Drive
Landover, MD 20785

Dan N. Hagedon
Pacific Northwest Laboratories
Battelle Boulevard
Richland, WA 99352

Dr. James Hannon
Lawrence Livermore National Laboratory
P.O. Box 808, L-205
Livermore, CA 94550

Dr. Roger Hansen
University of Colorado, JSPC
Campus Box 583
Boulder, CO 80309

Prof. David G. Harkrider
Division of Geological & Planetary Sciences
California Institute of Technology
Pasadena, CA 91125

Prof. Danny Harvey
University of Colorado, JSPC
Campus Box 583
Boulder, CO 80309

Prof. Donald V. Helmberger
Division of Geological & Planetary Sciences
California Institute of Technology
Pasadena, CA 91125

Prof. Eugene Herrin
Geophysical Laboratory
Southern Methodist University
Dallas, TX 75275

Prof. Robert B. Herrmann
Department of Earth & Atmospheric Sciences
St. Louis University
St. Louis, MO 63156

2

Prof. Lane R. Johnson
Seismographic Station
University of California
Berkeley, CA 94720

Prof. Thomas H. Jordan
Department of Earth, Atmospheric &
  Planetary Sciences
Massachusetts Institute of Technology
Cambridge, MA 02139

Prof. Alan Kafka
Department of Geology & Geophysics
Boston College
Chestnut Hill, MA 02167

Robert C. Kemerait
ENSCO, Inc.
445 Pineda Court
Melbourne, FL 32940

U.S. Dept of Energy
Max Koontz, NN-20, GA-033
Office of Research and Develop.
1000 Independence Avenue
Washington, DC 20585

Dr. Richard LaCoss
MIT Lincoln Laboratory, M-200B
P.O. Box 73
Lexington, MA 02173-0073

Dr. Fred K. Lamb
University of Illinois at Urbana-Champaign
Department of Physics
1110 West Green Street
Urbana, IL 61801

Prof. Charles A. Langston
Geosciences Department
403 Deike Building
The Pennsylvania State University
University Park, PA 16802

Jim Lawson, Chief Geophysicist
Oklahoma Geological Survey
Oklahoma Geophysical Observatory
P.O. Box 8
Leonard, OK 74043-0008

Prof. Thorne Lay
Institute of Tectonics
Earth Science Board
University of California, Santa Cruz
Santa Cruz, CA 95064

Dr. William Leith
U.S. Geological Survey
Mail Stop 928
Reston, VA 22092

Mr. James F. Lewkowicz
Phillips Laboratory/GPE
29 Randolph Road
Hanscom AFB, MA 01731-3010(2 copies)

Prof. L. Timothy Long
School of Geophysical Sciences
Georgia Institute of Technology
Atlanta, GA 30332

Dr. Randolph Martin, III
New England Research, Inc.
76 Olcott Drive
White River Junction, VT 05001

Dr. Robert Masse
Denver Federal Building
Box 25046, Mail Stop 967
Denver, CO 80225

Dr. Gary McCartor
Department of Physics
Southern Methodist University
Dallas, TX 75275

Prof. Thomas V. McEvilly
Seismographic Station
University of California
Berkeley, CA 94720

Dr. Art McGarr
U.S. Geological Survey
Mail Stop 977
U.S. Geological Survey
Menlo Park, CA 94025

Dr. Keith L. McLaughlin
S-CUBED
A Division of Maxwell Laboratory
P.O. Box 1620
La Jolla, CA 92038-1620

Stephen Miller & Dr. Alexander Florence
SRI International
333 Ravenswood Avenue
Box AF 116
Menlo Park, CA 94025-3493

Prof. Bernard Minster
IGPP, A-025
Scripps Institute of Oceanography
University of California, San Diego
La Jolla, CA 92093

Prof. Brian J. Mitchell
Department of Earth & Atmospheric Sciences
St. Louis University
St. Louis, MO 63156

Mr. Richard J. Morrow
USACDA/IVI
320 21st St. N.W.
Washington , DC 20451

Mr. Jack Murphy
S-CUBED
A Division of Maxwell Laboratory
11800 Sunrise Valley Drive, Suite 1212
Reston, VA 22091 (2 Copies)

Dr. Keith K. Nakanishi
Lawrence Livermore National Laboratory
L-025
P.O. Box 808
Livermore, CA 94550

Prof. John A. Orcutt
IGPP, A-025
Scripps Institute of Oceanography
University of California, San Diego
La Jolla, CA 92093

Prof. Jeffrey Park
Kline Geology Laboratory
P.O. Box 6666
New Haven, CT 06511-8130

Dr. Howard Patton
Lawrence Livermore National Laboratory
L-025
P.O. Box 808
Livermore, CA 94550

Dr. Frank Pilotte
HQ AFTAC/TT
1030 South Highway A1A
Patrick AFB, FL 32925-3002

Dr. Jay J. Pulli
Radix Systems, Inc.
201 Perry Parkway
Gaithersburg, MD 20877

Dr. Robert Reinke
ATTN: FCTVTD
Field Command
Defense Nuclear Agency
Kirtland AFB, NM 87115

Prof. Paul G. Richards
Lamont-Doherty Earth Observatory
   of Columbia University
Palisades, NY 10964

Mr. Wilmer Rivers
Teledyne Geotech
1300 17th St N #1450
Arlington, VA 22209-3803

Dr. Alan S. Ryall, Jr.
ARPA/NMRO
3701 North Fairfax Drive
Arlington, VA 22203-1714

Dr.Chandan K. Saikia
Woodward Clyde- Consultants
566 El Dorado Street
Pasadena, CA 91101

Dr. Richard Sailor
TASC, Inc.
55 Walkers Brook Drive
Reading, MA 01867

Prof. Charles G. Sammis
Center for Earth Sciences
University of Southern California
University Park
Los Angeles, CA 90089-0741

Prof. Christopher H. Scholz
Lamont-Doherty Earth Observatory
   of Columbia University
Palisades, NY 10964

Dr. Susan Schwartz
Institute of Tectonics
1156 High Street
Santa Cruz, CA 95064

Mr. Dogan Seber
Cornell University
Inst. for the Study of the Continent
3130 SNEE Hall
Ithaca, NY 14853-1504

Secretary of the Air Force
(SAFRD)
Washington, DC 20330

Office of the Secretary of Defense
DDR&E
Washington, DC 20330

Thomas J. Sereno, Jr.
Science Application Int'l Corp.
10260 Campus Point Drive
San Diego, CA 92121

Dr. Michael Shore
Defense Nuclear Agency/SPSS
6801 Telegraph Road
Alexandria, VA 22310

Dr. Robert Shumway
University of California Davis
Division of Statistics
Davis, CA 95616

Dr. Matthew Sibol
Virginia Tech
Seismological Observatory
4044 Derring Hall
Blacksburg, VA 24061-0420

Prof. David G. Simpson
IRIS, Inc.
1616 North Fort Myer Drive
Suite 1050
Arlington, VA 22209

Donald L. Springer
Lawrence Livermore National Laboratory
L-025
P.O. Box 808
Livermore, CA 94550

Dr. Jeffrey Stevens
S-CUBED
A Division of Maxwell Laboratory
P.O. Box 1620
La Jolla, CA 92038-1620

Prof. Brian Stump
Los Alamos National Laboratory
EES-3
Mail Stop C-335
Los Alamos, NM 87545

Prof. Jeremiah Sullivan
University of Illinois at Urbana-Champaign
Department of Physics
1110 West Green Street
Urbana, IL 61801

Prof. L. Sykes
Lamont-Doherty Earth Observatory
 of Columbia University
Palisades, NY 10964

Dr. David Taylor
ENSCO, Inc.
445 Pineda Court
Melbourne, FL 32940

Dr. Steven R. Taylor
Los Alamos National Laboratory
P.O. Box 1663
Mail Stop C335
Los Alamos, NM 87545

Prof. Tuncay Taymaz
Istanbul Technical University
Dept. of Geophysical Engineering
Mining Faculty
Maslak-80626, Istanbul Turkey

Prof. Clifford Thurber
University of Wisconsin-Madison
Department of Geology & Geophysics
1215 West Dayton Street
Madison, WS 53706

Prof. M. Nafi Toksoz
Earth Resources Lab
Massachusetts Institute of Technology
42 Carleton Street
Cambridge, MA 02142

Dr. Larry Turnbull
CIA-OSWR/NED
Washington, DC 20505

Dr. Gregory van der Vink
IRIS, Inc.
1616 North Fort Myer Drive
Suite 1050
Arlington, VA 22209

Dr. Karl Veith
EG&G
5211 Auth Road
Suite 240
Suitland, MD 20746

Prof. Terry C. Wallace
Department of Geosciences
Building #77
University of Arizona
Tuscon, AZ 85721

Dr. Thomas Weaver
Los Alamos National Laboratory
P.O. Box 1663
Mail Stop C335
Los Alamos, NM 87545

Dr. William Wortman
Mission Research Corporation
8560 Cinderbed Road
Suite 700
Newington, VA 22122

Prof. Francis T. Wu
Department of Geological Sciences
State University of New York
 at Binghamton
Vestal, NY 13901

Prof Ru-Shan Wu
University of California, Santa Cruz
Earth Sciences Department
Santa Cruz, CA 95064

ARPA, OASB/Library
3701 North Fairfax Drive
Arlington, VA 22203-1714

HQ DNA
ATTN: Technical Library
Washington, DC 20305

Defense Technical Information Center
Cameron Station
Alexandria, VA 22314 (2 Copies)

TACTEC
Battelle Memorial Institute
505 King Avenue
Columbus, OH 43201 (Final Report)

Phillips Laboratory
ATTN: XPG
29 Randolph Road
Hanscom AFB, MA 01731-3010

Phillips Laboratory
ATTN: GPE
29 Randolph Road
Hanscom AFB, MA 01731-3010

Phillips Laboratory
ATTN: TSML
5 Wright Street
Hanscom AFB, MA 01731-3004

Phillips Laboratory
ATTN: PL/SUL
3550 Aberdeen Ave SE
Kirtland, NM 87117-5776 (2 copies)

Dr. Michel Bouchon
I.R.I.G.M.-B.P. 68
38402 St. Martin D'Heres
Cedex, FRANCE

Dr. Michel Campillo
Observatoire de Grenoble
I.R.I.G.M.-B.P. 53
38041 Grenoble, FRANCE

Dr. Kin Yip Chun
Geophysics Division
Physics Department
University of Toronto
Ontario, CANADA

Prof. Hans-Peter Harjes
Institute for Geophysic
Ruhr University/Bochum
P.O. Box 102148
4630 Bochum 1, GERMANY

Prof. Eystein Husebye
NTNF/NORSAR
P.O. Box 51
N-2007 Kjeller, NORWAY

David Jepsen
Acting Head, Nuclear Monitoring Section
Bureau of Mineral Resources
Geology and Geophysics
G.P.O. Box 378, Canberra, AUSTRALIA

Ms. Eva Johannisson
Senior Research Officer
FOA
S-172 90 Sundbyberg, SWEDEN

Dr. Peter Marshall
Procurement Executive
Ministry of Defense
Blacknest, Brimpton
Reading FG7-FRS, UNITED KINGDOM

Dr. Bernard Massinon, Dr. Pierre Mechler
Societe Radiomana
27 rue Claude Bernard
75005 Paris, FRANCE (2 Copies)

Dr. Svein Mykkeltveit
NTNT/NORSAR
P.O. Box 51
N-2007 Kjeller, NORWAY (3 Copies)

Prof. Keith Priestley
University of Cambridge
Bullard Labs, Dept. of Earth Sciences
Madingley Rise, Madingley Road
Cambridge CB3 OEZ, ENGLAND

Dr. Jorg Schlittenhardt
Federal Institute for Geosciences & Nat'l Res.
Postfach 510153
D-30631 Hannover , GERMANY

Dr. Johannes Schweitzer
Institute of Geophysics
Ruhr University/Bochum
P.O. Box 1102148
4360 Bochum 1, GERMANY

Trust & Verify
VERTIC
Carrara House
20 Embankment Place
London WC2N 6NN, ENGLAND